response of GH to ghrelin requires the existence of GHRH (9). Kamegai et al. (13) reported that pituitary ghrelin regulates GH secretion by modulating pituitary response to GHRH. The decreased expression of GHS-R in pituitary in *db/db* and HFD mice might contribute to suppressed GH response to ghrelin by attenuating the pituitary response to GHRH. Of course, decreased mRNA levels of GH in pituitary or, as reported in human (6, 16), elevated serum IGF-I or FFA levels in these mice might also contribute to suppressed GH responses.

Although GH responses to ghrelin were also decreased in Akita mice, the pituitary mRNA levels of GHS-R were significantly higher than those seen in control mice, indicating that pituitary GHS-R did not contribute to decreased GH responses. GHRH mRNA expression levels in hypothalamus of Akita mice were significantly lower compared with those of control mice. This reduction of GHRH mRNA levels may be responsible for decreased GH responses to ghrelin in Akita mice. Ghrelin stimulates GHRH secretion from the hypothalamus (27). And recently, Mano-Otagiri et al. (17) reported that GHS-R signaling upregulates hypothalamic GHRH expression. Although plasma ghrelin levels were significantly higher in Akita mice than those displayed by control mice, GHRH mRNA expression levels in hypothalamus of Akita mice were significantly decreased. In addition, the food intake of Akita mice was significantly elevated at baseline and was not stimulated by ghrelin any further. These results indicate the existence of ghrelin unresponsiveness in postreceptor level in hypothalamus.

In the chronic treatment experiment, ghrelin and GHRH treatment for 10 days tended to stimulate food intake and showed fat-sparing effect in control mice. In contrast, HFD mice injected with ghrelin and GHRH tended to decrease more fat mass compared with those treated with saline, which may be due to restored GH secretion and suppressed orexigenic response to ghrelin. In this setting, blood glucose and serum insulin levels did not change by ghrelin and GHRH treatment in HFD mice. This may be explained by the fact that the change in fat mass was only subtle and that lean body mass did not change by ghrelin and GHRH treatment. These results indicate that low-dose ghrelin and GHRH supplementation at least do not worsen obesity and metabolic status and that it may at least partially restore suppressed GH secretion.

In the current experiment, IGF-I levels were higher in HFD mice after chronic treatment of ghrelin and GHRH. Since IGF-I levels of the saline-treated group of HFD mice were also higher than those of control mice, this elevation seems to reflect nutritional status between HFD and control mice.

In conclusion, we demonstrated that acute GH responses to ghrelin were suppressed in both genetic and diet-induced mouse models of obesity. The decreased pituitary levels of GHS-R mRNA may contribute to suppression of GH response. We also demonstrated that acute GH responses to ghrelin were suppressed in Akita mice, an insulin-deprived diabetic mouse model. Decreased GHRH mRNA levels in hypothalamus and the lack of stimulation of food intake by ghrelin indicate the involvement of hypothalamus in the mechanism of suppressed GH response to ghrelin in Akita mice. These results indicate that suppressed GH response to ghrelin has a different mechanism in obese and insulin-resistant mice and insulin-deprived diabetic animals. In addition, HFD mice injected with ghrelin and GHRH showed potentiated GH responses. Chronic treatment of low-dose ghrelin and GHRH did not promote fat deposition in HFD mice. These results indicate that low-dose ghrelin and GHRH administration at least does not worsen obesity and that it may restore suppressed GH secretion.

ACKNOWLEDGMENTS

We thank Hitomi Hiratani, Chieko Ishimoto, Naoko Takehisa, Kozue Fukuda, and Chinami Shiraiwa for excellent technical assistance.

GRANTS

This study was supported by funds from the Ministry of Education, Culture, Sports, Science, and Technology of Japan and the Ministry of Health, Labour, and Welfare of Japan.

REFERENCES

1. **Akamizu T, Shinomiya T, Irako T, Fukunaga M, Nakai Y, Kangawa K.** Separate measurement of plasma levels of acylated and desacyl ghrelin in healthy subjects using a new direct ELISA assay. *J Clin Endocrinol Metab* 90: 6–9, 2005.
2. **Alvarez-Castro P, Isidro ML, Garcia-Buela J, Leal-Cerro A, Broglio F, Tassone F, Ghigo E, Dieguez C, Casanueva FF, Cordido F.** Marked GH secretion after ghrelin alone or combined with GH-releasing hormone (GHRH) in obese patients. *Clin Endocrinol (Oxf)* 61: 250–255, 2004.
3. **Argente J, Caballo N, Barrios V, Pozo J, Munoz MT, Chowen JA, Hernandez M.** Multiple endocrine abnormalities of the growth hormone and insulin-like growth factor axis in prepubertal children with exogenous obesity: effect of short- and long-term weight reduction. *J Clin Endocrinol Metab* 82: 2076–2083, 1997.
4. **Arvat E, Di Vito L, Broglio F, Papotti M, Muccioli G, Dieguez C, Casanueva FF, Deghenghi R, Camanni F, Ghigo E.** Preliminary evidence that Ghrelin, the natural GH secretagogue (GHS)-receptor ligand, strongly stimulates GH secretion in humans. *J Endocrinol Invest* 23: 493–495, 2000.
5. **Broglio F, Arvat E, Benso A, Gottero C, Muccioli G, Papotti M, van der Lely AJ, Deghenghi R, Ghigo E.** Ghrelin, a natural GH secretagogue produced by the stomach, induces hyperglycemia and reduces insulin secretion in humans. *J Clin Endocrinol Metab* 86: 5083–5086, 2001.
6. **Cordido F, Fernandez T, Martinez T, Penalva A, Peino R, Casanueva FF, Dieguez C.** Effect of acute pharmacological reduction of plasma free fatty acids on growth hormone (GH) releasing hormone-induced GH secretion in obese adults with and without hypopituitarism. *J Clin Endocrinol Metab* 83: 4350–4354, 1998.
7. **Cutfield WS, Wilton P, Bennmarker H, Albertsson-Wikland K, Chatelain P, Ranke MB, Price DA.** Incidence of diabetes mellitus and impaired glucose tolerance in children and adolescents receiving growth-hormone treatment. *Lancet* 355: 610–613, 2000.
8. **Date Y, Murakami N, Kojima M, Kuroiwa T, Matsukura S, Kangawa K, Nakazato M.** Central effects of a novel acylated peptide, ghrelin, on growth hormone release in rats. *Biochem Biophys Res Commun* 275: 477–480, 2000.
9. **Fintini D, Alba M, Schally AV, Bowers CY, Parlow AF, Salvatori R.** Effects of combined long-term treatment with a growth hormone-releasing hormone analogue and a growth hormone secretagogue in the growth hormone-releasing hormone knock out mouse. *Neuroendocrinology* 82: 198–207, 2005.
10. **Furuhata Y, Kagaya R, Hirabayashi K, Ikeda A, Chang KT, Nishihara M, Takahashi M.** Development of obesity in transgenic rats with low circulating growth hormone levels: involvement of leptin resistance. *Eur J Endocrinol* 143: 535–541, 2000.
11. **Giustina A, Veldhuis JD.** Pathophysiology of the neuroregulation of growth hormone secretion in experimental animals and the human. *Endocr Rev* 19: 717–797, 1998.
12. **Iwakura H, Hosoda K, Son C, Fujikura J, Tomita T, Noguchi M, Ariyasu H, Takaya K, Masuzaki H, Ogawa Y, Hayashi T, Inoue G, Akamizu T, Hosoda H, Kojima M, Itoh H, Toyokuni S, Kangawa K, Nakao K.** Analysis of rat insulin II promoter-ghrelin transgenic mice and rat glucagon promoter-ghrelin transgenic mice. *J Biol Chem* 280: 15247–15256, 2005.
13. **Kamegai J, Tamura H, Shimizu T, Ishii S, Tatsuguchi A, Sugihara H, Oikawa S, Kineman RD.** The role of pituitary ghrelin in growth hormone (GH) secretion: GH-releasing hormone-dependent regulation of pituitary

ghrelin gene expression and peptide content. *Endocrinology* 145: 3731–3738, 2004.

14. **Kojima M, Hosoda H, Date Y, Nakazato M, Matsuo H, Kangawa K.** Ghrelin is a growth-hormone-releasing acylated peptide from stomach. *Nature* 402: 656–660, 1999.
15. **Luque RM, Kineman RD.** Impact of obesity on the growth hormone (GH)-axis: evidence for a direct inhibitory effect of hyperinsulinemia on pituitary function. *Endocrinology* 147: 2754–2763, 2006.
16. **Maccario M, Tassone F, Gianotti L, Lanfranco F, Grottoli S, Arvat E, Muller EE, Ghigo E.** Effects of recombinant human insulin-like growth factor I administration on the growth hormone (gh) response to GH-releasing hormone in obesity. *J Clin Endocrinol Metab* 86: 167–171, 2001.
17. **Mano-Otagiri A, Nemoto T, Sekino A, Yamauchi N, Shuto Y, Sugihara H, Oikawa S, Shibasaki T.** Growth hormone-releasing hormone (GHRH) neurons in the arcuate nucleus (Arc) of the hypothalamus are decreased in transgenic rats whose expression of ghrelin receptor is attenuated: evidence that ghrelin receptor is involved in the up-regulation of GHRH expression in the arc. *Endocrinology* 147: 4093–4103, 2006.
18. **Masuda Y, Tanaka T, Inomata N, Ohnuma N, Tanaka S, Itoh Z, Hosoda H, Kojima M, Kangawa K.** Ghrelin stimulates gastric acid secretion and motility in rats. *Biochem Biophys Res Commun* 276: 905–908, 2000.
19. **Nagaya N, Uematsu M, Kojima M, Ikeda Y, Yoshihara F, Shimizu W, Hosoda H, Hirota Y, Ishida H, Mori H, Kangawa K.** Chronic administration of ghrelin improves left ventricular dysfunction and attenuates development of cardiac cachexia in rats with heart failure. *Circulation* 104: 1430–1435, 2001.
20. **Nakazato M, Murakami N, Date Y, Kojima M, Matsuo H, Kangawa K, Matsukura S.** A role for ghrelin in the central regulation of feeding. *Nature* 409: 194–198, 2001.
21. **Poykko SM, Kellokoski E, Horkko S, Kauma H, Kesaniemi YA, Ukkola O.** Low plasma ghrelin is associated with insulin resistance, hypertension, and the prevalence of type 2 diabetes. *Diabetes* 52: 2546–2553, 2003.
22. **Shintani M, Ogawa Y, Ebihara K, Aizawa-Abe M, Miyanaga F, Takaya K, Hayashi T, Inoue G, Hosoda K, Kojima M, Kangawa K, Nakao K.** Ghrelin, an endogenous growth hormone secretagogue, is a novel orexigenic peptide that antagonizes leptin action through the activation of hypothalamic neuropeptide Y/Y1 receptor pathway. *Diabetes* 50: 227–232, 2001.
23. **Takaya K, Ariyasu H, Kanamoto N, Iwakura H, Yoshimoto A, Harada M, Mori K, Komatsu Y, Usui T, Shimatsu A, Ogawa Y, Hosoda K, Akamizu T, Kojima M, Kangawa K, Nakao K.** Ghrelin strongly stimulates growth hormone release in humans. *J Clin Endocrinol Metab* 85: 4908–4911, 2000.
24. **Tschop M, Smiley DL, Heiman ML.** Ghrelin induces adiposity in rodents. *Nature* 407: 908–913, 2000.
25. **Tschop M, Weyer C, Tataranni PA, Devanarayan V, Ravussin E, Heiman ML.** Circulating ghrelin levels are decreased in human obesity. *Diabetes* 50: 707–709, 2001.
26. **Veldhuis JD, Iranmanesh A, Ho KK, Waters MJ, Johnson ML, Lizarralde G.** Dual defects in pulsatile growth hormone secretion and clearance subserve the hyposomatotropism of obesity in man. *J Clin Endocrinol Metab* 72: 51–59, 1991.
27. **Wren AM, Small CJ, Fribbens CV, Neary NM, Ward HL, Seal LJ, Ghatei MA, Bloom SR.** The hypothalamic mechanisms of the hypophysiotropic action of ghrelin. *Neuroendocrinology* 76: 316–324, 2002.
28. **Wren AM, Small CJ, Ward HL, Murphy KG, Dakin CL, Taheri S, Kennedy AR, Roberts GH, Morgan DG, Ghatei MA, Bloom SR.** The novel hypothalamic peptide ghrelin stimulates food intake and growth hormone secretion. *Endocrinology* 141: 4325–4328, 2000.
29. **Yoshioka M, Kayo T, Ikeda T, Koizumi A.** A novel locus, Mody4, distal to D7Mit189 on chromosome 7 determines early-onset NIDDM in nonobese C57BL/6 (Akita) mutant mice. *Diabetes* 46: 887–894, 1997.

Am J Physiol Renal Physiol 293: F1363–F1372, 2007.
First published August 15, 2007; doi:10.1152/ajprenal.00205.2007.

Expression of CCN1 (CYR61) in developing, normal, and diseased human kidney

Kazutomo Sawai,[1,6] Masashi Mukoyama,[1] Kiyoshi Mori,[1] Masato Kasahara,[1] Masao Koshikawa,[1] Hideki Yokoi,[1] Tetsuro Yoshioka,[1] Yoshihisa Ogawa,[1] Akira Sugawara,[1] Hiroyuki Nishiyama,[2] Shigehito Yamada,[3] Takashi Kuwahara,[4] Moin A. Saleem,[5] Kohei Shiota,[3] Osamu Ogawa,[2] Mikiya Miyazato,[6] Kenji Kangawa,[6] and Kazuwa Nakao[1]

Departments of [1]Medicine and Clinical Science and [2]Urology, and [3]Congenital Anomaly Research Center, Kyoto University Graduate School of Medicine, Kyoto; [4]Department of Nephrology, Osaka Saiseikai Nakatsu Hospital, Osaka; [5]Children's Renal Unit, University of Bristol, Bristol, United Kingdom; [6]Department of Biochemistry, National Cardiovascular Center Research Institute, Osaka, Japan

Submitted 30 April 2007; accepted in final form 6 August 2007

Sawai K, Mukoyama M, Mori K, Kasahara M, Koshikawa M, Yokoi H, Yoshioka T, Ogawa Y, Sugawara A, Nishiyama H, Yamada S, Kuwahara T, Saleem MA, Shiota K, Ogawa O, Miyazato M, Kangawa K, Nakao K. Expression of CCN1 (CYR61) in developing, normal, and diseased human kidney. *Am J Physiol Renal Physiol* 293: F1363–F1372, 2007. First published August 15, 2007; doi:10.1152/ajprenal.00205.2007.—CCN1 (cysteine-rich protein 61; Cyr61) is an extracellular matrix-associated signaling molecule that functions in cell migration, adhesion, and differentiation. We previously reported that CCN1 is induced at podocytes in rat anti-Thy-1 glomerulonephritis, a well-known model of reversible glomerular injury, but its expression and significance in the human kidney remain totally unknown (Sawai K, Mori K, Mukoyama M, Sugawara A, Suganami T, Koshikawa M, Yahata K, Makino H, Nagae T, Fujinaga Y, Yokoi H, Yoshioka T, Yoshimoto A, Tanaka I, Nakao K. *J Am Soc Nephrol* 14: 1154–1163, 2003). Here we report that, in the human kidney, CCN1 expression was confined to podocytes in normal adult and embryonic glomeruli from the capillary loop stage. Podocyte CCN1 expression was decreased in IgA nephropathy, diabetic nephropathy, and membranous nephropathy, whereas it remained unchanged in minimal change disease and focal segmental glomerulosclerosis. Downregulation of CCN1 was significantly greater in diseased kidneys with severe mesangial expansion. CCN1 protein was also localized in the thick ascending limb of Henle's loop, distal and proximal tubules, and collecting ducts, which was not altered in diseased kidneys. In vitro, recombinant CCN1 protein enhanced endothelial cell adhesion, whereas it prominently inhibited mesangial cell adhesion. CCN1 also completely suppressed mesangial cell migration, suggesting its role as a mesangial-repellent factor. In cultured podocytes, CCN1 markedly induced the expression of cyclin-dependent kinase inhibitor $p27^{Kip1}$ as well as synaptopodin in a dose-dependent manner and suppressed podocyte migration. These data indicate that CCN1 is expressed in podocytes, can act on glomerular cells to modulate glomerular remodeling, and is downregulated in diseased kidneys, suggesting that impairment of CCN1 expression in podocytes may contribute to the progression of glomerular disease with mesangial expansion.

podocyte; glomerular visceral epithelial cell; cysteine-rich protein 61; mesangial cell; synaptopodin

CYSTEINE-RICH PROTEIN 61 (Cyr61; also known as CCN1) is a secreted, 42-kDa, angiogenic protein belonging to the family of CCN proteins, which contains Cyr61 (CCN1), connective tissue growth factor (CTGF; CCN2), nephroblastoma overexpressed (Nov; CCN3), and Wnt-induced secreted proteins (WISP)-1, -2, and -3 (CCN4, 5, and 6, respectively) (3, 19, 28). CCN proteins are associated with extracellular matrix, interact with various integrins, and mediate a variety of biological actions including cell adhesion, migration, and differentiation, and induce angiogenesis both in vitro and in vivo (2, 3, 13, 19, 28). Among them, CCN1 is essential for vessel bifurcation during development, and most CCN1-null mice suffer embryonic death between embryonic (E) days *E11.5* and *E14.5* due to vessel malformation in the placenta and within embryos (22). In adults, CCN1 is suggested to be involved in skin wound healing (4) and adaptation to cardiovascular stress such as ischemia and pressure overload (11), but its role in the kidney remains undefined.

We have recently reported that CCN1 is prominently induced at podocytes during glomerular regeneration in rat anti-Thy-1 glomerulonephritis (Thy-1 GN) (32), a well-known model of reversible glomerulonephritis. CCN1 expression in podocytes was potently stimulated by transforming growth factor-β (TGF-β) and platelet-derived growth factor (PDGF) (32). CCN1 was also expressed in the proximal straight tubules, where its expression was not altered during Thy-1 GN. Conditioned medium from CCN1-overexpressing cells inhibited mesangial cell migration without affecting cell proliferation (32). From these results, we speculated that CCN1 secreted from podocytes might enhance glomerular repair in Thy-1 GN by protecting the glomerular capillary lumen from being occluded by migrating mesangial cells. However, the expression and the pathophysiological significance of CCN1 in human kidneys remain to be elucidated.

In this study, we investigated CCN1 expression in fetal and adult human kidneys, as well as in various glomerular diseases. Furthermore, we studied the effects of CCN1 on mesangial cells and podocytes in vitro. Our data indicate that CCN1 expression in podocytes is decreased in diseased kidneys with mesangial expansion, suggesting that impairment of CCN1 expression may contribute to the progression of various glomerular diseases.

Address for reprint requests and other correspondence: M. Mukoyama, Dept. of Medicine and Clinical Science, Kyoto Univ. Graduate School of Medicine, 54 Shogoin Kawahara-cho, Sakyo-ku, Kyoto 606-8507, Japan (e-mail: muko@kuhp.kyoto-u.ac.jp).

The costs of publication of this article were defrayed in part by the payment of page charges. The article must therefore be hereby marked "*advertisement*" in accordance with 18 U.S.C. Section 1734 solely to indicate this fact.

Table 1. *Clinical parameters of the patients*

Diagnosis	*n*	Gender (M/F)	Age, yr	sCr, mg/dl	BUN, mg/dl	Urinary Protein, g/g Cr	C_{cr}, ml/min
Normal adult human kidney (control)	12	2/10	55±6	0.70±0.04	14.8±1.2	0.06±0.02	100±11
Nephrectomy	7	2/5	68±5	0.79±0.04	16.9±1.3	0.04±0.01	95±23
Minor glomerular abnormalities	5	0/5	36±8	0.58±0.04	11.8±1.6	0.08±0.03	103±9
Human fetal kidney	10	5/5		ND	ND	ND	ND
IgAN	33	16/17	37±3	0.98±0.10*	15.6±1.4	0.86±0.16‡	84±5
MCNS	7	3/4	39±3	0.77±0.07	13.7±1.8	10.0±2.76‡	96±9
FSGS	9	6/3	57±2	1.23±0.14†	26.8±5.7	2.17±0.79‡	50±8*
MN	8	3/5	59±1	0.73±0.07	12.3±1.6	2.18±0.48‡	80±6
DN	29	22/7	59±2	1.35±0.12†	24.2±2.0*	6.14±0.96‡	55±9†

Values are means ± SE. *n*, No. of patients; sCr, serum creatinine; BUN, blood urea nitrogen; C_{cr}, creatinine clearance; IgAN, IgA nephropathy; MCNS, minimal change nephrotic syndrome; FSGS, focal segmental glomerulosclerosis; MN, membranous nephropathy; DN, diabetic nephropathy; ND, not determined. *$P < 0.05$, †$P < 0.005$, and ‡$P < 0.0005$ vs. control.

MATERIALS AND METHODS

Patients and tissue samples. Needle renal biopsy tissues were obtained from 86 patients treated at Kyoto University Hospital or Saiseikai Nakatsu Hospital with various glomerulopathies: 33 with IgA nephropathy (IgAN), 29 with type 2 diabetic nephropathy (DN), 7 with minimal change nephrotic syndrome (MCNS), 9 with focal segmental glomerulosclerosis (FSGS), and 8 with membranous nephropathy (MN). Diagnosis was confirmed by pathological evaluation of specimens, such as light microscopy, electron microscopy, and immunofluorescence staining. No patients received steroids or immunosuppressive drugs before biopsy. Ten human fetal kidneys (estimated gestational age ranging from 16 to 20 wk) were obtained fresh from tissues examined after therapeutic abortion at the Congenital Anomaly Research Center, Kyoto University Graduate School of Medicine. For normal controls, tissues obtained from seven patients afflicted with localized neoplasm using uninvolved portions of surgically removed kidneys and five biopsy samples from patients with minor glomerular abnormalities were used. Histopathological examination of control tissues excluded any glomerular diseases. This study was approved by the Ethics Committee of Kyoto University Graduate School of Medicine, and informed consent was obtained in accordance with protocols approved by the committee.

After resecting, the samples were fixed in Dubosq-Brazil solution. Table 1 summarizes details of the analyzed materials. Patients with IgAN were further classified as those with mild mesangial expansion (*group I*) and with severe mesangial expansion (*group II*), defined as a mesangial area <30% (*group I*) and >30% (*group II*) of total glomerular area, respectively. Clinical parameters of IgAN between two groups are summarized in Table 2.

Immunohistochemical analysis. Immunohistochemical analysis was performed as previously described with some modifications (32, 33). In brief, deparaffinized 3-μm kidney sections were treated with autoclave heating, and specimens were incubated with 1% Triton X-100 (Nacalai Tesque, Kyoto, Japan) in PBS for 20 min, washed three times with PBS, and incubated with 10% normal donkey serum in PBS for 10 min at room temperature. Goat antibody against the COOH terminus of human Cyr61 (CCN1; sc-8561, Santa Cruz Biotechnology, Santa Cruz, CA) or rabbit anti-human Wilms' tumor-1 (WT1) antibody (sc-192, Santa Cruz Biotechnology) was diluted 1:50 in PBS containing 1% BSA (1% BSA/PBS) and incubated for 1 h at room temperature. After blocking of endogenous phosphatase with 2 mM levamisole, the sections were incubated with alkaline phosphatase-conjugated donkey anti-goat or anti-rabbit IgG (Jackson ImmunoResearch, West Grove, PA) in 1% BSA/PBS for 30 min at room temperature. The sections were processed with NBT-BCIT (Roche Diagnostics, Mannheim, Germany) in alkaline buffer (100 mM Tris, pH 9.5, 100 mM NaCl, 50 mM $MgCl_2$) and counterstained with Kernechtrot stain solution (Muto Pure Chemicals, Tokyo, Japan). For double staining, the sections were pretreated with 3% hydrogen peroxide for 15 min at room temperature, incubated with peroxidase-conjugated secondary antibody against rabbit IgG (Jackson ImmunoResearch), and processed with 3,3′-diaminobenzidine tetrahydrochloride (Kanto Chemical, Tokyo, Japan). Nonimmune goat or rabbit serum was used as negative control.

Histological and morphometric analysis. Staining intensity of CCN1 and WT1 in kidney samples was examined by two independent investigators, and the score was averaged. At least six glomeruli per biopsy were evaluated at high-power magnification, and the intensity was semiquantified by a rating of 0–3 (most prominent). The number of CCN1- and WT1-positive cells per glomerular cross section was quantified as described elsewhere (33). Mesangial area was computer analyzed by measuring the periodic acid-Schiff (PAS)-positive area in cross sections of glomeruli scanned from vascular poles, using an automatic image analyzer (KS400, Carl Zeiss Vision, Munich, Germany) (35). To analyze CCN1 expression in cultured human podocytes, cells were fixed with 3.7% formaldehyde for 20 min followed by permeabilization with 0.1% Triton X-100 for 20 min at room temperature. After being rinsed with PBS, primary antibody anti-Cyr61 (CCN1; sc-8561, Santa Cruz Biotechnology) was applied for 60 min at room temperature. Antigen-antibody complexes were visualized using FITC-conjugated secondary antibody (705–095-147, Jackson ImmunoResearch). Confocal fluorescence microscopy was done with a laser-scanning microscope (Fluoview FV500, Olympus, Tokyo, Japan) with appropriate filters.

Purification of recombinant CCN. Conditioned media of Sf9 cells (Invitrogen, Carlsbad, CA) infected with baculovirus driving the

Table 2. *Clinical parameters of IgAN patients with mild (Group I) and severe (Group II) mesangial expansion*

	Gender (M/F)	Age, yr	sCr, mg/dl	BUN, mg/dl	Urinary Protein, g/g Cr	C_{cr}, ml/min	Mesangial Area (% of Total Glomerular Area)
Group I (*n* = 21)	11/10	30±2	0.85±0.06	13.5±1.2	0.58±0.13	96±4	26.0±1.2
Group II (*n* = 12)	5/7	42±5	1.28±0.20	19.1±3.2	1.42±0.31	62±9	37.1±1.5
P value, *group I* vs. *group II*		NS	NS	NS	$P < 0.05$	$P < 0.05$	$P < 0.0001$

Values are means ± SE. IgAN were classified into 2 groups defined as those with mesangial area <30% (*group I*) and >30% (*group II*) of total glomerular area, respectively. NS, not significantly different.

synthesis of CCN1 were used as a source for purification, as previously described (13). Full-length mouse CCN1 cDNA was generated by RT-PCR using total RNA from C57BL/6 mouse kidneys, and the following primers were used: sense, 5′-tgcgcgccacaatgagctccagca-3′ and antisense, 5′-ttagtccctgaacttgtggatgtc-3′ (nucleotides 179–1329, GenBank accession number M32490) (18). CCN1 cDNA was TA-cloned into pGEM-T Easy vector (Promega, Madison, WI) and transferred into pBacPAK vector (Clontech, Palo Alto, CA). The transfer vector along with BacPAK6 viral DNA (Clontech) was delivered into cells by liposome-mediated transfection to obtain a recombinant virus. Sf9 cells grown to 10^6 cells/ml in SFM-II medium were infected with the recombinant virus and incubated for 48 h at 28°C. The conditioned media centrifuged at 5,000 *g* for 5 min at 4°C were adjusted to 50 mM sodium phosphate buffer (pH 6.0) containing 2 mM EDTA and 1 mM PMSF and applied to a Hitrap SP column (Amersham, Piscataway, NJ) at 4°C. The column was washed with the same buffer containing 150 mM NaCl, and bound protein was subsequently eluted with a stepwise gradient of NaCl (0.2–1.0 M) in 50 mM sodium phosphate buffer (pH 6.0). The fractions were analyzed by 10% SDS-PAGE followed by Coomassie brilliant blue (Nacalai) staining or Western blotting. Fractions containing CCN1 were combined and adjusted to pH 7.5 with 0.5 M Tris·HCl/10% glycerol before storage in aliquots at −80°C. Protein concentration was determined by the modified Bradford method with a protein assay kit (Bio-Rad, Hercules, CA).

Cell culture. Human umbilical vein endothelial cells (HUVEC; Clonetics, Walkersville, MD) were maintained in the basal medium with growth supplements (EGM-2; Clonetics) containing 2% FCS (Cansera International, Ontario, Canada). Cell cultures between *passages 5* and *7* were used for each experiment. Mesangial cells established from glomeruli of 6-wk-old Sprague-Dawley rats were cultured in DMEM (Invitrogen) containing 10% FCS and antibiotics (32) and used between *passages 7* and *10*. Human mesangial cells (Clonetics) were maintained in the basal medium with growth supplements (CC-3147; Clonetics). Cell cultures between *passages 5* and *8* were used for each experiment.

Conditionally immortalized mouse podocytes (a kind gift from Dr. Peter Mundel) were cultured with RPMI 1640 medium (Nihonseiyaku, Tokyo, Japan) containing 10% FCS and antibiotics on dishes coated with type I collagen (Koken, Tokyo, Japan) as described elsewhere (24, 32). The cells proliferate when cultured at 33°C with 10 U/ml IFN-γ (Life Technologies, Gaithersburg, MD), whereas they halt growing and begin to differentiate when cultured at 37°C without IFN-γ. For CCN1 stimulation experiments, cells were differentiated for 2 wk and cultured with RPMI 1640/1% FCS for 24 h, until stimulation with recombinant CCN1 for 24 h on collagen I-coated dishes (Iwaki Glass, Chiba, Japan). Cells were used between *passages 15* and *20*. Conditionally immortalized human podocytes were cultured as described previously (33). These cells proliferate when cultured at 33°C, whereas they halt growing when cultured at 37°C. Cells were cultured

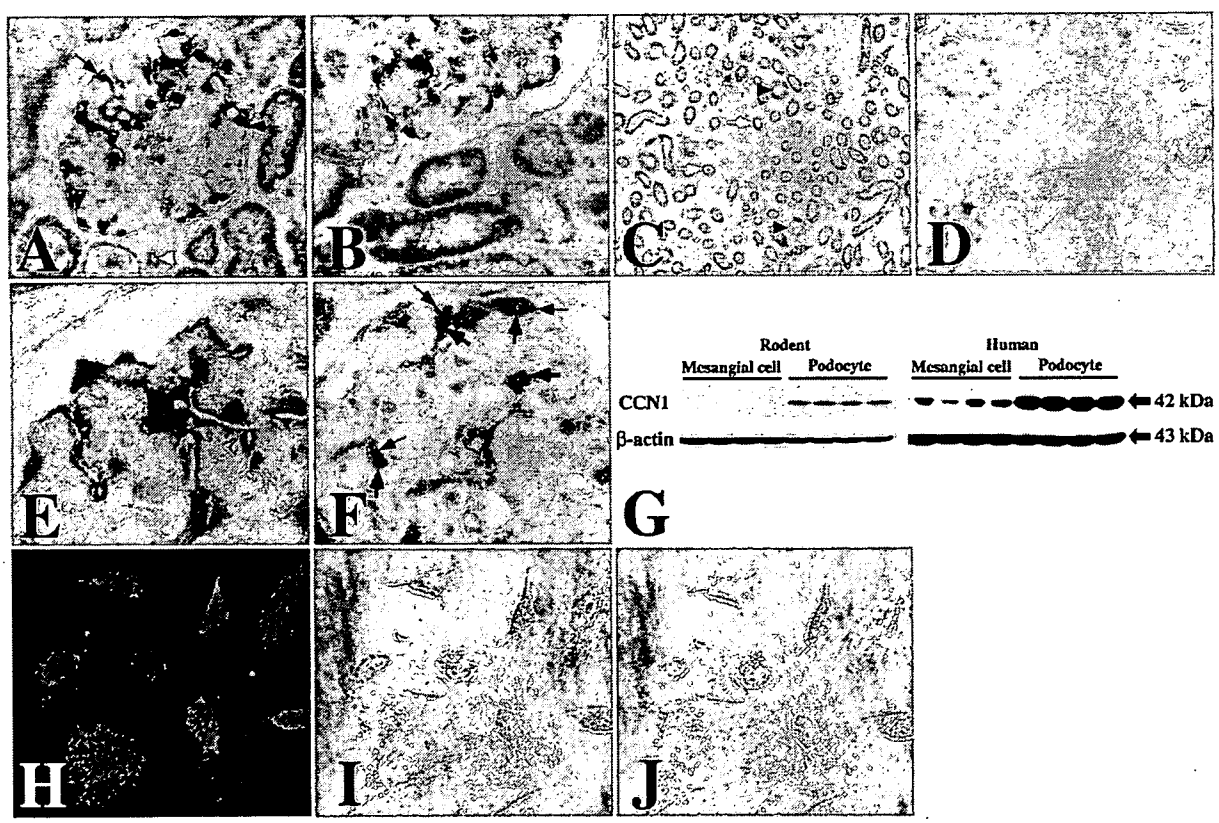

Fig. 1. Immunohistochemical analyses of cysteine-rich protein 61 (Cyr61; CCN1) expression in normal adult human kidney. CCN1 expression was detected at podocytes exclusively within the glomeruli (*A* and *F*, black arrows). CCN1-positive cells (*F*, black arrows) were also positive for WT1 (*F*, brown arrows). Weak CCN1 expression was also observed in some of arterioles (*A*, white arrowhead). Parietal epithelial cells, mesangial cells, and endothelial cells were negative for CCN1 in the glomeruli (*A*, *E*, and *F*). CCN1 expression was localized to the distal and proximal tubules (*B*), the thick ascending limb of Henle's loop (*C*, white arrows), and collecting ducts (*C*, black arrowheads). There was no detectable CCN1 expression within endothelial cells or smooth muscle cell of arteries (*D*). Cultured mouse and human podocytes significantly expressed a higher level of CCN1 compared with cultured rat and human mesangial cells, respectively (*G*). Confocal fluorescence microscopy revealed both cytoplasmic and nuclear expression of CCN1 (*H* and *J*, green) in human cultured podocytes (*I*, counterphase of *H*; *J*, merged image of *H* and *I*). Magnification: ×400 (*A*, *B*, *D*, *H–J*); ×200 (*C*); ×1,000 (*E* and *F*).

with RPMI 1640 medium (Sigma-Aldrich) supplemented with 10% FCS (Sigma-Aldrich) and an insulin-transferrin-sodium selenite media supplement (Sigma-Aldrich) on tissue culture dish (Corning, Corning, NY). Cells were differentiated at 37°C for 2 wk without passage and were subcultured on 96-well plates (146520, Nunc, Roskilde, Denmark). Cells were used between *passages 15* and *18*. For CCN1 expression analysis, cells grown at 33°C were used.

Northern and Western blot analyses. Northern blot analysis was performed as described elsewhere (32). In brief, after RNA extraction by TRIzol Reagent (Invitrogen), total RNA (20 μg in each lane) was electrophoresed on 1.0% agarose gels and transferred to nylon membranes (GeneScreen Plus, NEN, Boston, MA). The cDNA fragments of mouse synaptopodin (nucleotides 2165–2766, GenBank accession number XM_619543), mouse podocalyxin (nucleotides 1184–1601, GenBank accession number AF290209), mouse podoplanin (nucleotides 420–809, GenBank accession number BC026551), and mouse α-actinin-4 (nucleotides 2425–2809, GenBank accession number NM_021895) were generated by RT-PCR and used as probes. The membranes were hybridized with [^{32}P]dCTP-labeled probes, and the blots were exposed to a BAS-III imaging plate. The amount of RNA loaded in each lane was normalized for 28S ribosomal RNA.

Western blot analysis was performed as described elsewhere (16, 33). In brief, cells were lysed on ice in solution containing 20 mM Tris·HCl (pH 7.5), 12 mM glycerophosphate, 0.1 M EGTA, 1 mM pyrophosphate, 5 mM NaF, 5 mg/ml aprotinin, 2 mM dithiothreitol, 1 mM PMSF, 1% Triton X-100, and 1 mM sodium orthovanadate (Sigma-Aldrich). The lysate was centrifuged at 15,000 *g* for 20 min at 4°C, and the samples mixed with Laemmli's sample buffer were separated by 12.5% SDS-PAGE and transferred onto Immobilon filters (Millipore, Bedford, MA). The filters were incubated with rabbit anti-p27 (sc-528, Santa Cruz Biotechnology), goat anti-Cyr61 (CCN1; sc-8561, Santa Cruz Biotechnology), or mouse anti-β actin antibodies (A5441, Sigma-Aldrich) diluted in Block Ace (Snow Brand Milk Products, Sapporo, Japan) for 2 h at room temperature and were developed with horseradish peroxidase-conjugated donkey secondary antibodies (Santa Cruz Biotechnology) and a chemiluminescence kit (ECL plus, Amersham).

Cell adhesion assay. Adhesion of HUVEC and mesangial cells was analyzed using 96-well microtiter plates (Corning) coated with increasing concentrations of CCN1 protein diluted in PBS at 50 μl/well, followed by blocking with 1% BSA (14). For HUVEC, subconfluent cells were washed twice with PBS/1 mM EDTA/0.1% glucose and harvested by incubation in the same buffer for 15 min at room temperature. Cells were washed and resuspended in serum-free basal medium containing 0.2% BSA/10 mM HEPES (pH 7.2) at 4 × 10^6 cells/ml. The cell suspension was plated at 50 μl/well and allowed to adhere to protein-coated wells at 37°C for 20 min, followed by washing twice with PBS. Adherent cells were fixed with 10% formalin and stained with 1% methylene blue in 10 mM boric acid buffer (pH 8.5). Adhesion was quantified by measuring absorbance at 620 nm (14). For mesangial cells, subconfluent cells were washed twice with PBS and harvested by incubation in 0.1% trypsin/EDTA. Cells resuspended in DMEM/1.0% FCS at 10^6 cells/ml were plated at 50 μl/well and allowed to adhere to wells at 37°C for 50 min, followed by washing twice with PBS. Adherent cells were fixed and quantified as above.

Cell migration assay. Migration of mesangial cells and podocytes was analyzed by a modified Boyden chamber method using 96-well chambers (Neuro Probe, Gaithersburg, MD) as described elsewhere (4, 32). Polycarbonate filters (8 μm) coated with poly-L-lysine (Sigma-Aldrich) for mesangial cells, or type I collagen for podocytes, were placed in the middle of the chambers. Cells suspended in medium with 1% FCS (10^5 cells/well) were placed in the top chambers. CCN1 protein in medium with 1% FCS with or without PDGF-BB was added to the bottom chambers. After incubation for 3 h at 37°C, the cells that had migrated to the lower surface were fixed in methanol, stained with 0.5% Coomassie brilliant blue in 50% methanol/40% water/10% acetic acid, and quantified by measuring absorbance at 620 nm.

Statistical analysis. Results are given as means ± SE. A Mann-Whitney *U*-test was used to compare unpaired two-group means. Statistical analysis was performed with a Stat View (R) software package (Abacus, Berkeley, CA), and the difference with $P < 0.05$ was considered statistically significant.

RESULTS

CCN1 expression in normal adult human kidney. The immunohistochemical staining pattern of CCN1 in normal adult kidneys was essentially consistent in the 12 samples analyzed (Fig. 1, summarized in Table 3). Within the glomeruli, podocytes were invariably positive for CCN1 staining, whereas parietal epithelial cells, mesangial cells, and endothelial cells were virtually negative for CCN1 (Fig. 1*A*). Podocytes were identified morphologically as cells located at the outer aspect of the glomerular basement membrane (GBM) and immunohistochemically as WT1-positive cells (Fig. 1*F*). CCN1 expression in podocytes was detected mainly in the cytoplasm and also in the nucleus (Fig. 1, *A* and *E*). In tubular epithelial cells,

Table 3. *Summary of CCN1 expression in the adult kidney*

Cell Type	Normal	IgAN	MCNS	FSGS	MN	DN
Glomerulus						
Mesangial cells	−	−	−	−	−	−
Visceral epithelial cells (podocytes)						
Cytoplasm	+++	−~++	++~+++	++~+++	±~++	−~±
Nucleus	+++	−~++	++~+++	++~+++	±~++	+~+++
Parietal epithelial cells	−	−	−	−	−	−
Capillary endothelial cells	−	−	−	−	−	−
Vasculature						
Endothelial cells	−	−	−	−	−	−
Smooth muscle cells	−	−	−	−	−	−
Adventitial cells	−	−	−	−	−	−
Tubulointerstitium						
Proximal tubules	++	++	++	++	++	++
Distal tubules	++	++	++	++	++	++
Loop of Henle	+++	+++	+++	+++	+++	+++
Collecting ducts	++	++	++	++	++	++
Interstitial cells	−	−	−	−	−	−

CCN1, cysteine-rich protein 61.

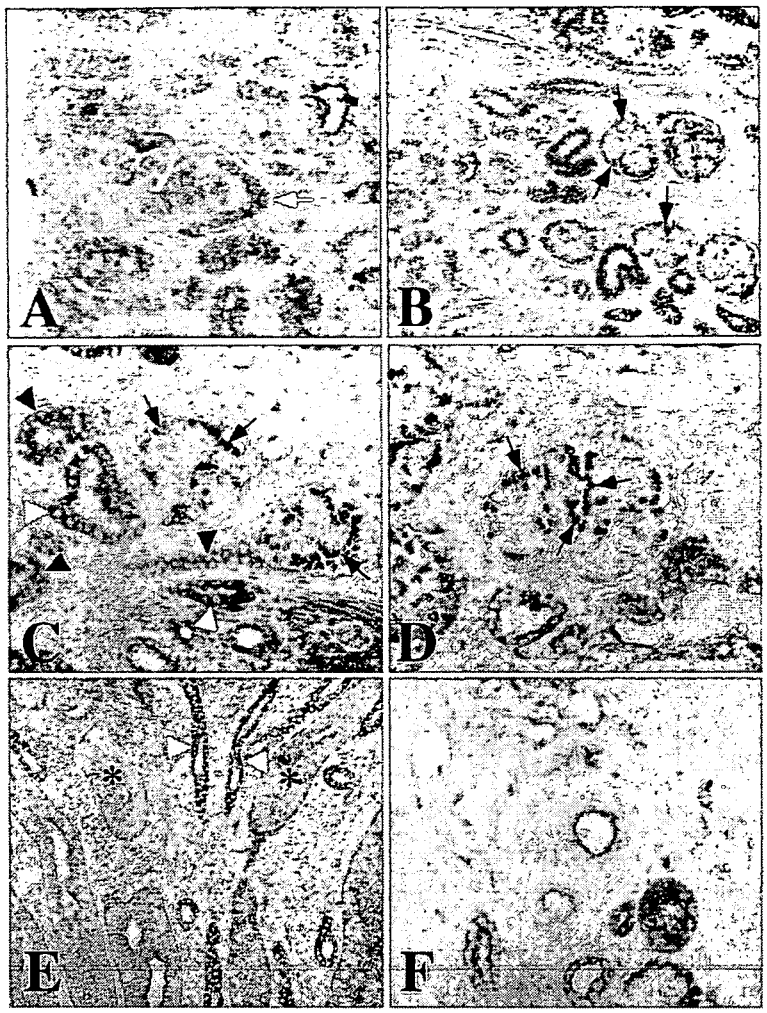

Fig. 2. Immunohistochemical analyses of CCN1 expression in fetal human kidney. CCN1 was negative or faintly positive in early glomerular stages (*A*, white arrow). From the late capillary loop stage, CCN1 expression was detected in developing podocytes (*B–D*, black arrows). There was also CCN1 expression in developing thick ascending limb of Henle's loop, distal tubules (*C* and *E*, white arrowheads), proximal tubules (*C*, black arrowheads), and collecting ducts (*E*, asterisks). CCN1 was also detected at endothelial cells in arteries and arterioles (*F*). Magnification: ×400 (*A*, *C*, and *F*); ×200 (*B* and *E*); ×1,000 (*D*).

CCN1 staining was positive in the thick ascending limb of Henle's loop, distal tubules, proximal tubules, and collecting ducts (Fig. 1, *B* and *C*). CCN1 expression in the tubular cells was prominent in the cytoplasm, and to a lesser extent in the nucleus (Fig. 1, *B* and *C*). Weak expression of CCN1 protein was also observed in some of afferent and efferent arterioles (Fig. 1*A*), but the protein was not expressed in larger vessels (Fig. 1*D*). Negative controls with nonimmune goat or rabbit serum gave no staining in all analyzed normal and diseased kidneys (data not shown). Compatible with human kidney tissue, cultured podocytes expressed abundant CCN1 compared with mesangial cells (Fig. 1*G*). Confocal fluorescence microscopy revealed both cytoplasmic and nuclear expression of CCN1 in human cultured podocytes (Fig. 1, *H–J*).

CCN1 expression in developing human kidney. In the developing human kidneys, CCN1 showed a distinct localization pattern (Fig. 2, summarized in Table 4). In early glomerular stages, i.e., comma-shaped and S-shaped bodies, CCN1 was almost completely negative in the glomeruli (Fig. 2, *A* and *B*). From the late capillary loop stage, CCN1 expression was detected in the glomeruli, restricted to the developing podocytes (Fig. 2, *B–D*). CCN1 expression in fetal podocytes was detected mainly in the nucleus and also in the cytoplasm (Fig. 2*D*). Intensity of CCN1 expression in podocytes was stronger in glomeruli at the maturing stage (Fig. 2, *B* and *C*). Other glomerular cell types, including developing endothelial cells, mesangial cells, and parietal epithelial cells, were uniformly

Table 4. *Expression of CCN1 in the fetal kidney*

Site	CCN1 Expression
Glomerulus	
Comma-shaped body	−
S-shaped body	−
Capillary loop stage	Visceral epithelial cells (podocytes) +~++
Maturing-stage glomeruli	Visceral epithelial cells (podocytes) ++~+++
Tubules	
Distal tubules	+++
Thick ascending limb of Henle	+++
Proximal tubules	++
Collecting ducts	+
Vasculature	
Arterial endothelial cells	+
Smooth muscle cells	−

negative for CCN1 (Fig. 2*D*). Strong CCN1 expression was detected in the developing thick ascending limb of Henle's loop, distal tubules, and proximal tubules (Fig. 2, *C* and *E*). Weak expression was present in developing collecting ducts (Fig. 2*E*). In the vasculature, CCN1 was detected at endothelial cells in arteries and arterioles (Fig. 2*F*).

CCN1 expression in IgAN. The CCN1 staining pattern was studied in 33 specimens with IgAN (Fig. 3, summarized in Tables 1–3). Cases included minimal lesions, those with mesangial hypercellularity and/or mesangial expansion, and those with severe focal necrosis and crescents (represented in Fig. 3, *F*, *H*, and *J*, respectively). In cases with IgAN, glomerular CCN1 expression was also confined to podocytes (Fig. 3, *C*, *E*, *G*, and *I*) as in normal glomeruli (Fig. 3*A*). WT1 staining in the nucleus as a podocyte marker in adjacent sections confirmed podocyte-specific expression of CCN1 (Fig. 3, *A–D*). In IgAN, however, the intensity of CCN1 staining in podocytes was decreased in various degrees compared with normal controls (Fig. 3*M*). Furthermore, some podocytes seemed to have lost CCN1 expression (Fig. 3, *C* and *E*). In contrast, WT1 staining intensity was not reduced in IgAN (Fig. 3*M*). Closer examination revealed that expression of CCN1 was markedly decreased in podocytes surrounding glomerular tufts with severe mesangial expansion (Fig. 3*G*) and in those adjacent to segmental sclerosis (Fig. 3*I*). Thus CCN1 staining intensity at podocytes was significantly reduced in cases with severe mesangial expansion (*group II*) compared with those with mild mesangial lesion (*group I*) (Fig. 3*N*, Table 2). The number of CCN1-positive cells per glomerulus was also significantly decreased in *group II* (Fig. 3*N*). Tubular CCN1 expression and its localization were well preserved in IgAN, even in tubular cells with advanced tubulointerstitial lesion (Fig. 3, *K* and *L*).

CCN1 expression in other glomerular diseases. Next, we evaluated cases with MCNS, FSGS, MN, and DN as glomer-

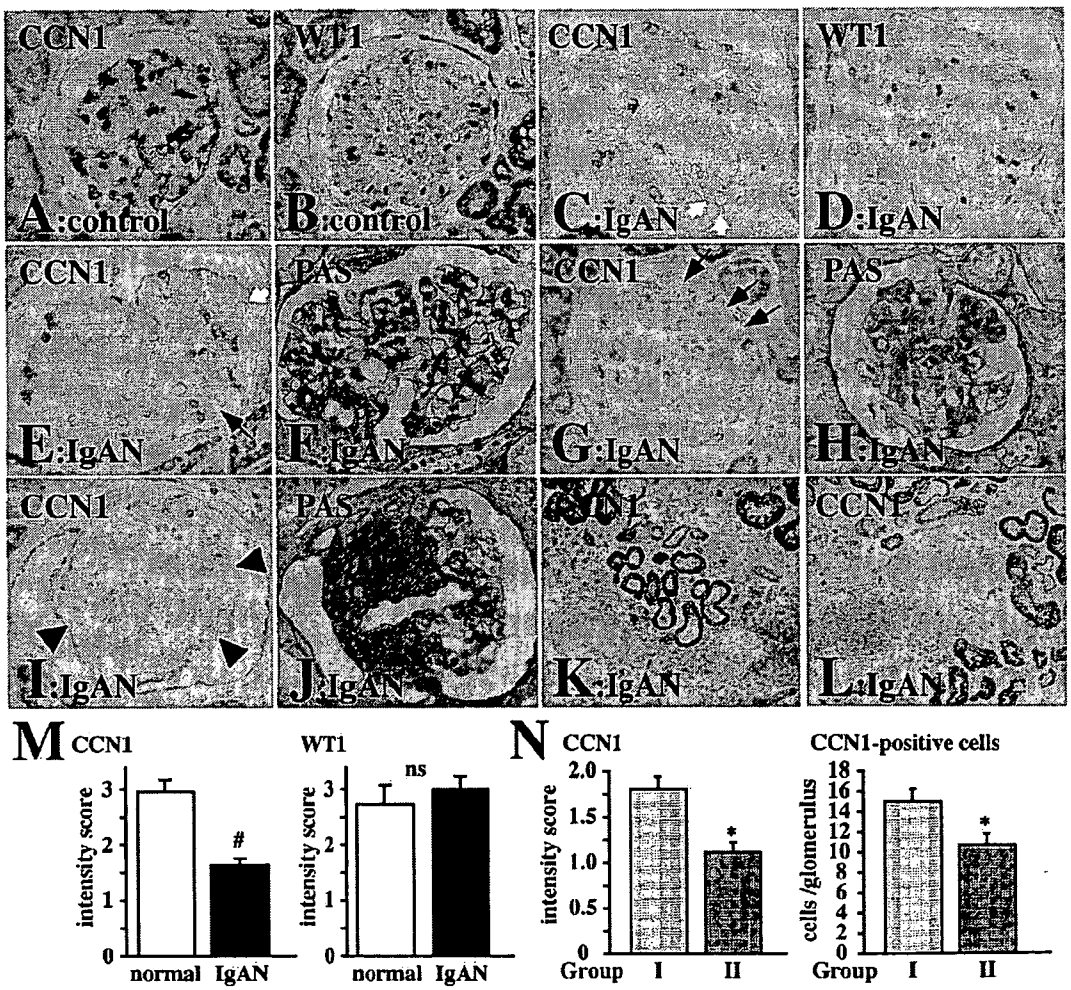

Fig. 3. CCN1 expression in IgA nephropathy (IgAN). CCN1 staining (*A*, *C*, *E*, *G*, *I*, *K*, *L*), WT1 staining (*B* and *D*), and periodic acid-Schiff (PAS) staining (*F*, *H*, and *J*) of renal biopsy specimens from patients with IgAN (*C–L*) and normal controls (*A* and *B*) is shown. Compared with normal controls (*A*), CCN1 staining intensity at podocytes was decreased in IgAN (*C*, *E*, *G*, and *I*). Expression of CCN1 was downregulated especially in podocytes surrounding the glomerular tuft with mesangial expansion (*G*, black arrows), and in podocytes next to segmental sclerosis (*I*, black arrowheads). CCN1-negative podocytes were frequently observed (white arrows). CCN1 expression was well preserved in the tubular cells (*K* and *L*). Intensity of CCN1 expression in podocytes was significantly decreased in IgAN compared with normal controls, whereas intensity of Wilms' tumor-1 (WT1) was not altered (*M*). Decrease in CCN1 intensity and the number of CCN1-positive cells was prominent in IgAN with severe mesangial expansion (*group II*) compared with those with only mild mesangial expansion (*group I*; *N*). ns, Not significantly different. Magnification: ×400 (*A–J*); ×200 (*K* and *L*). #$P < 0.005$ vs. normal control. *$P < 0.005$ vs. *group I*.

ular disease with various degrees of mesangial expansion (Fig. 4, summarized in Table 3). CCN1 expression was also confined to podocytes in these glomerulopathies (Fig. 4, *C*, *E*, *G*, and *I*). In cases with MCNS or FSGS, the intensity of CCN1 expression in podocytes was decreased in some glomeruli, but not with statistical significance (Fig. 4, *C*, *E*, and *K*). Podocyte CCN1 expression was significantly decreased in cases with MN (Fig. 4, *G* and *K*), and also in DN, which had a prominent decrease in cytoplasmic CCN1 (Fig. 4, *I* and *K*, Table 3). CCN1-positive cells per glomerular cross section were decreased in all of the glomerular diseases examined, which in part may be due to a loss of podocytes, indicated by decreased WT1-positive cells per glomerular cross section (Fig. 4*L*). However, the ratio of CCN1-positive cells to WT1-positive cells was significantly decreased in IgAN by 23% but was not altered in MCNS, FSGS, MN, and DN (Fig. 4*L*). CCN1-negative podocytes frequently seen in IgAN were not observed in these glomerular diseases. WT1 staining intensity was not altered in any of these diseases (Fig. 4, *D*, *F*, *H*, *J*, and K). Tubular CCN1 was preserved in MCNS, FSGS, MN, and DN (data not shown), as was the case with IgAN (Fig. 3, *K* and *L*).

Effects of CCN1 on mesangial cell adhesion and migration. To clarify the functional role of CCN1 expressed at podocytes, effects of recombinant CCN1 protein were examined in vitro. Because CCN1 expression at podocytes was decreased in glomeruli with mesangial expansion, we examined the effects of CCN1 on mesangial adhesion and migration. Although CCN1 significantly augmented endothelial cell attachment (Fig. 5*A*) as in previous reports (13, 14), CCN1 caused a marked inhibition of mesangial cell adhesion (Fig. 5*A*). Next, we examined the effect of CCN1 on mesangial migration. In the presence of PDGF-BB, CCN1 potently abolished PDGF-induced mesangial migration (Fig. 5*B*). These results show that CCN1 can act on mesangial cells as a potential inhibitor of adhesion and migration.

Effects of CCN1 on podocyte differentiation. To explore the role of CCN1 on podocytes, podocytes cultured under differ-

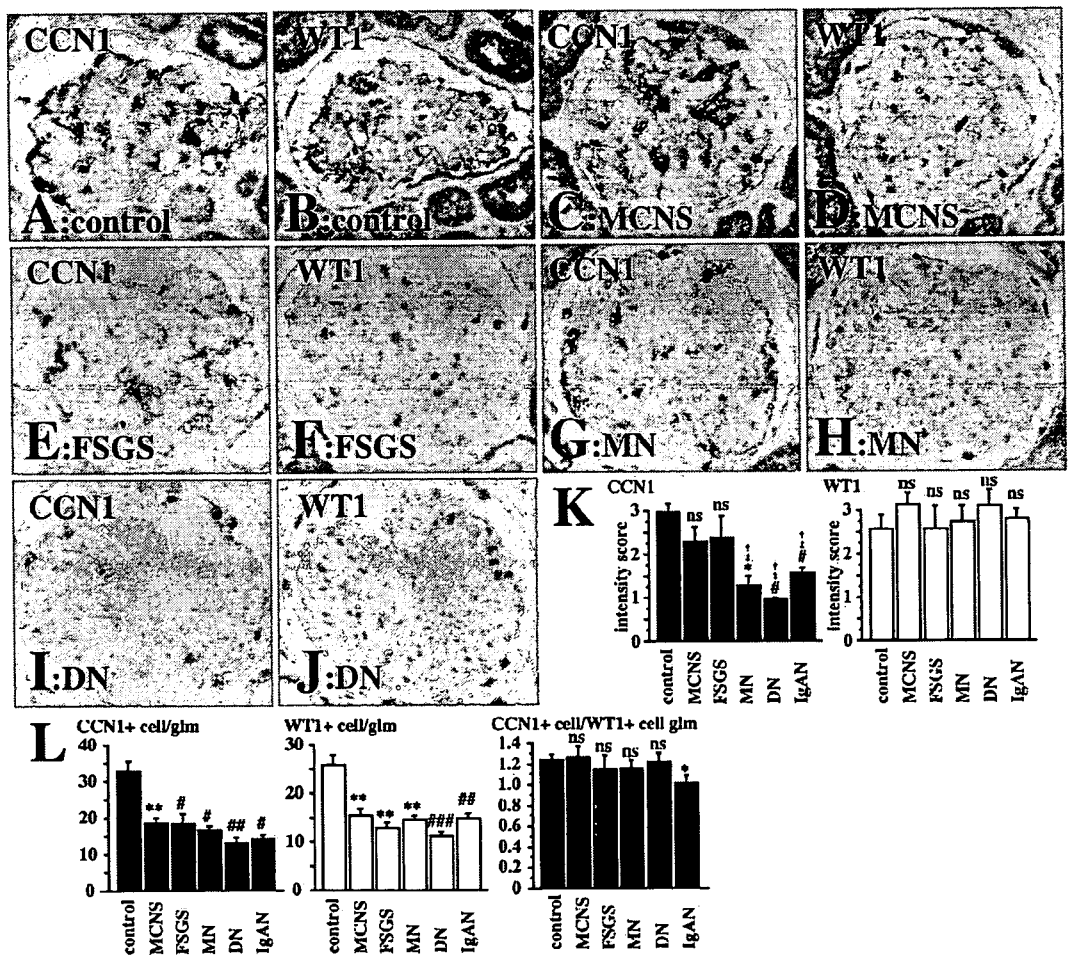

Fig. 4. CCN1 expression in minimal change nephrotic syndrome (MCNS), focal segmental glomerulosclerosis (FSGS), membranous nephropathy (MN), and diabetic nephropathy (DN). CCN1 staining (*A*, *C*, *E*, *G*, and *I*) and WT1 staining (*B*, *D*, *F*, *H*, and *J*) of normal controls (*A* and *B*), MCNS (*C* and *D*), FSGS (*E* and *F*), MN (*G* and *H*), and DN (*I* and *J*) is shown. CCN1 expression in podocyte cytoplasm was significantly decreased in MN and DN compared with normal controls, MCNS, and FSGS (*A*, *C*, *E*, *G*, *I*, and *K*), whereas the intensity of WT1 in podocytes was not altered (*B*, *D*, *F*, *H*, *J*, and *K*). CCN1-positive cells as well as WT1-positive cells per glomerular cross section (glm) were decreased in all of the glomerular diseases examined, and the ratio of CCN1-positive cells to WT1-positive cells was significantly decreased in IgAN (*L*). Magnification: ×400 (*A–J*). $*P < 0.05$ vs. normal control. $**P < 0.01$ vs. normal control. $\#P < 0.005$ vs. normal control. $\#\#P < 0.001$ vs. normal control. $\#\#\#P < 0.0005$ vs. normal control. $\dagger P < 0.05$ vs. MCNS. $\ddagger P < 0.05$ vs. FSGS.

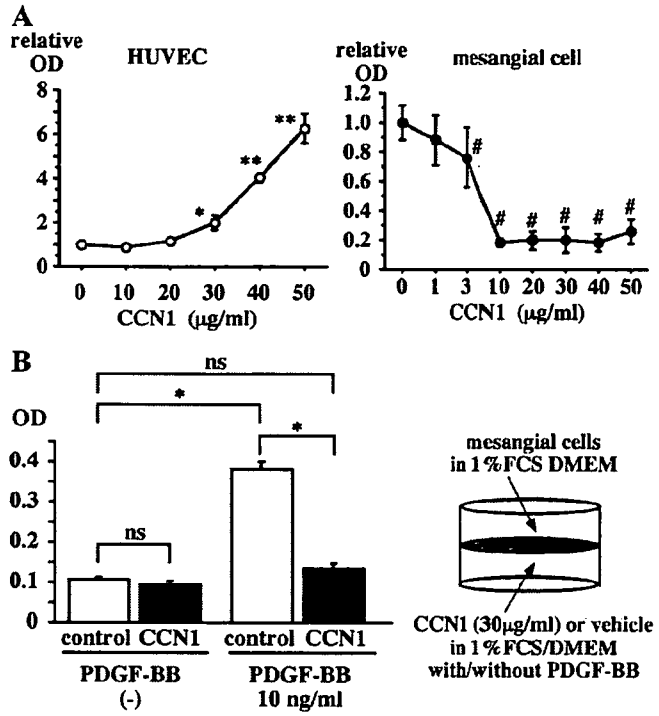

Fig. 5. Effects of CCN1 on mesangial cell adhesion and migration. Purified CCN1 protein enhanced adhesion of human umbilical vein endothelial cells (HUVEC) but potently inhibited mesangial cell adhesion (*A*). Recombinant CCN1 showed almost complete inhibition of PDGF-induced migration at 30 μg/ml (*B*). $*P < 0.05$, $**P < 0.005$, and $\#P < 0.01$ vs. control; $n = 5$–6.

entiating condition for 2 wk were incubated with recombinant CCN1 for an additional 24 h. Synaptopodin, a marker widely used to identify differentiated phenotypes of podocytes, was upregulated dose dependently (Fig. 6, *A* and *C*). Other podocyte-specific genes including podocalyxin, podoplanin, and α-actinin-4, were not significantly induced by addition of CCN1. Since differentiation of podocytes leads to a quiescent phenotype both in vitro and in vivo (5, 25, 34), we examined the effect of CCN1 on $p27^{Kip1}$ (p27) expression, a cyclin-dependent kinase inhibitor (CKI) involved in the maintenance of G0/G1 phase arrest in podocytes (5). CCN1 upregulated p27 protein dose dependently (4.2-fold with 3 μg/ml CCN1) (Fig. 6, *B* and *C*). Because the migratory phenotype of podocytes is reported to be involved in glomerulosclerosis (17, 30, 31), we finally examined the effect of CCN1 on podocyte migration. CCN1 significantly suppressed podocyte migration by 26% (Fig. 6*D*). Thus CCN1 may act as an autocrine/paracrine factor, promoting podocyte differentiation and maintaining its quiescent phenotype.

DISCUSSION

In the present study, we investigated CCN1 protein expression in normal fetal and adult human kidneys and those with various nephropathies. In normal glomeruli, CCN1 was predominantly expressed at podocytes from the capillary loop stage to mature glomeruli. CCN1 was also present in the thick ascending limb of Henle's loop, distal and proximal tubules, and collecting ducts. Decrease in CCN1 expression at podocytes was observed in IgAN, DN, and MN. Especially in IgAN, CCN1-negative podocytes were frequently observed, and the intensity of CCN1 staining at podocytes was significantly reduced in cases with severe mesangial expansion. In vitro, CCN1 prominently inhibited adhesion and migration of mesangial cells. Furthermore, CCN1 induced p27 and synaptopodin expression, indicating that CCN1 may act as an autocrine factor to stimulate podocyte differentiation.

CCN1 at podocytes may exert its function in two ways: one in a secreted form, and the other as a factor inside the nucleus. Secreted CCN1, which may be quantified by CCN1 staining at the cytoplasm, can act on glomerular cells in a GBM-bound form, since CCN1 has a high affinity for heparan sulfate proteoglycans (37), a major component of the GBM (8). Furthermore, CCN1 interacts with a variety of integrins (3, 9, 14, 19, 28), e.g., acting through integrin $\alpha_v\beta_3$ on endothelial cells and through $\alpha_v\beta_5$ on fibroblasts (9, 14), both of which are expressed in mesangial cells and podocytes (10). It was recently reported that production of vascular endothelial growth factor A, a homodimeric glycoprotein of 48 kDa, from podocytes is required for mesangial cell survival in vivo (6), suggesting that secreted factors from podocytes can act on glomerular cells, counteracting against the flow from the capillary lumen to the urinary space. It is therefore likely that CCN1, an extracellular matrix-associated protein with a similar molecular weight, secreted from podocytes can either act on

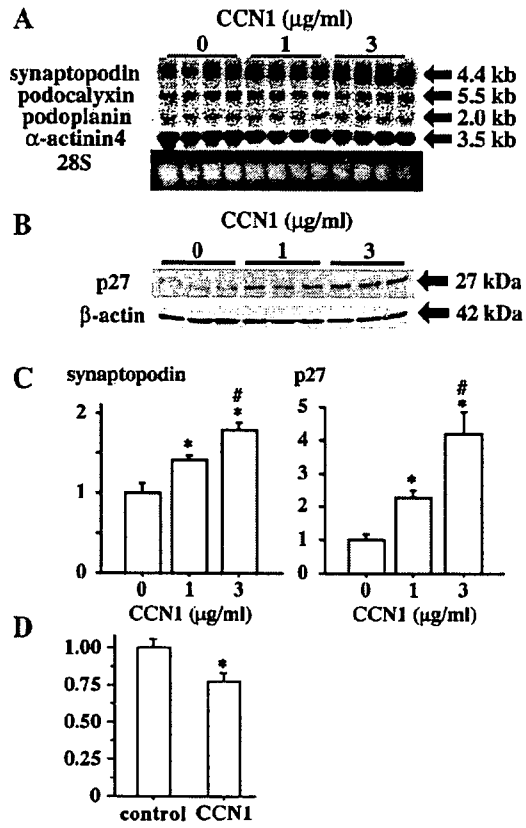

Fig. 6. Effects of CCN1 on cultured podocytes. Recombinant CCN1 enhanced the expression of synaptopodin mRNA (*A*) and cyclin-dependent kinase inhibitor p27 protein (*B*) in a dose-dependent manner (*C*). Podocyte migration was significantly suppressed by addition of CCN1 at 3 μg/ml (*D*). $*P < 0.05$ vs. 0 μg/ml. $\#P < 0.05$ vs. 1 μg/ml; $n = 4$.

themselves in an autocrine manner or act on mesangial cells as a GBM-bound form, through integrin complexes on these cells.

Podocytes are terminally differentiated, quiescent cells, possessing well-developed processes, and express podocyte-specific proteins such as WT1 and synaptopodin (27). In contrast, typical "dedifferentiated" podocytes proliferate and have decreased synaptopodin expression (17). Abnormal podocyte function, such as dedifferentiation, loss, or inflammatory change, is postulated to play a central role in nephron degeneration (17). Therefore it is important to understand the underlying mechanisms, but very few factors are known to be involved in the maintenance of podocytes at differentiated phenotypes (7, 12, 21, 36). In this study, we revealed that CCN1 upregulates synaptopodin expression in vitro and showed that CCN1 is induced in vivo at the capillary loop stage, when synaptopodin is first detected during kidney development. Synaptopodin is essential for podocyte foot process formation, by blocking the actin-branching activity of α-actinin-4 to develop unbranched actin bundles (1). Our observation that CCN1 upregulated synaptopodin, but not α-actinin-4, implies the role of CCN1 in podocyte foot process formation, which needs to be clarified in the future studies.

CKIs maintain G0/G1 cell cycle arrest in mature podocytes, and their downregulation is responsible for podocyte proliferation in pathological conditions (5, 25, 34). We showed in this study that CCN1 enhances the expression of CKI p27 in vitro and that CCN1 is upregulated in vivo at the capillary loop stage, when p27 is also induced in the developing kidney (5, 25). Decreased CCN1 expression at podocytes in IgAN may contribute to downregulation of podocyte p27, as reported previously in proliferative IgAN (29).

A decrease in the ratio of CCN1-positive cells to WT1-positive cells was prominent in IgAN, indicating the appearance of CCN1-negative podocytes in IgAN. In fact, CCN1-negative podocytes were frequently observed in IgAN. CCN1-negative podocytes may contribute to the pathological lesion seen in IgAN in two ways: first, a decrease in GBM-bound CCN1 may enhance mesangial migration, which leads to glomerular tuft occlusion and to glomerulosclerosis. Second, excessive podocyte migration can lead to podocyte bridging, and further on to glomerular crescent formation (17, 20, 23, 26, 30, 31). The functional significance of CCN1 downregulation in IgAN should await further clarification.

Downregulation of CCN1 at podocytes may be merely a consequence of podocyte loss or damage, but we assume it unlikely for the following reasons. First, we found that WT1 expression intensity was not altered despite a dramatic change in CCN1 expression in podocytes. Second, a reduction in CCN1 expression at podocytes was significant in IgAN, DN, and MN compared with MCNS and FSGS. Since MCNS and FSGS are supposed to have more pronounced podocyte damage compared with IgAN (15), it is unlikely that podocyte damage alone leads to CCN1 downregulation. Third, the findings that podocyte CCN1 expression is decreased in glomeruli with overt mesangial expansion, and that CCN1 is markedly downregulated at podocytes adjacent to mesangial expansion or segmental sclerosis, supports the possible mesangial-repellent activity of CCN1. Taken together, we hypothesize that decreased CCN1 expression in podocytes may, at least in part, play a role in disease progression in these glomerulopathies.

In conclusion, we show that CCN1, which acts as a potential mesangial-repellent factor and a podocyte differentiation factor, is predominantly expressed by podocytes in glomeruli of adult human kidneys and that CCN1 expression at podocytes is downregulated in various diseases associated with mesangial expansion. Although the functional relevance is still unclarified, these findings raise the possibility that impairment of CCN1 expression at podocytes may play a role in the progression of various human glomerulopathies.

ACKNOWLEDGMENTS

The authors gratefully acknowledge Dr. Peter Mundel (Mount Sinai School of Medicine, New York, NY) for the immortalized mouse podocyte cell line and Dr. Peter W. Mathieson (University of Bristol, Bristol, UK) for the immortalized human podocyte cell line; Dr. Lester F. Lau (University of Illinois at Chicago) and Dr. K. Nagahama for discussions; C. Uwabe, J. Nakamura, and S. Saito for technical assistance; and A. Sonoda and S. Doi for secretarial assistance. We also acknowledge the contribution of collaborating obstetricians.

GRANTS

This work was supported in part by research grants from the Japanese Ministry of Education, Culture, Sports, Science and Technology and the Japanese Ministry of Health, Labour, and Welfare.

REFERENCES

1. **Asanuma K, Kim K, Oh J, Giardino L, Chabanis S, Faul C, Reiser J, Mundel P.** Synaptopodin regulates the actin-bundling activity of alpha-actinin in an isoform-specific manner. *J Clin Invest* 115: 1188–1198, 2005.
2. **Babic AM, Kireeva ML, Kolesnikova TV, Lau LF.** CYR61, a product of a growth factor-inducible immediate early gene, promotes angiogenesis and tumor growth. *Proc Natl Acad Sci USA* 95: 6355–6360, 1998.
3. **Brigstock DR.** The connective tissue growth factor/cysteine-rich 61/nephroblastoma overexpressed (CCN) family. *Endocr Rev* 20: 189–206, 1999.
4. **Chen CC, Mo FE, Lau LF.** The angiogenic factor Cyr61 activates a genetic program for wound healing in human skin fibroblasts. *J Biol Chem* 276: 47329–47337, 2001.
5. **Combs HL, Shankland SJ, Setzer SV, Hudkins KL, Alpers CE.** Expression of the cyclin kinase inhibitor, p27kip1, in developing and mature human kidney. *Kidney Int* 53: 892–896, 1998.
6. **Eremina V, Cui S, Gerber H, Ferrara N, Haigh J, Nagy A, Ema M, Rossant J, Jothy S, Miner JH, Quaggin SE.** Vascular endothelial growth factor A signaling in the podocyte-endothelial compartment is required for mesangial cell migration and survival. *J Am Soc Nephrol* 17: 724–735, 2006.
7. **Griffin SV, Hiromura K, Pippin J, Petermann AT, Blonski MJ, Krofft R, Takahashi S, Kulkarni AB, Shankland SJ.** Cyclin-dependent kinase 5 is a regulator of podocyte differentiation, proliferation, and morphology. *Am J Pathol* 165: 1175–1185, 2004.
8. **Groffen AJ, Veerkamp JH, Monnens LA, van den Heuvel LP.** Recent insights into the structure and functions of heparan sulfate proteoglycans in the human glomerular basement membrane. *Nephrol Dial Transplant* 14: 2119–2129, 1999.
9. **Grzeszkiewicz TM, Kirschling DJ, Chen N, Lau LF.** CYR61 stimulates human skin fibroblast migration through integrin $\alpha_v\beta_5$ and enhances mitogenesis through integrin $\alpha_v\beta_3$ independent of its carboxyl-terminal domain. *J Biol Chem* 276: 21943–21950, 2001.
10. **Hafdi Z, Lesavre P, Nejjari M, Halbwachs-Mecarelli L, Droz D, Noel LH.** Distribution of alphavbeta3, alphavbeta5 integrins and the integrin associated protein–IAP (CD47) in human glomerular diseases. *Cell Adhes Commun* 7: 441–451, 2000.
11. **Hilfiker-Kleiner D, Kaminski K, Kaminska A, Fuchs M, Klein G, Podewski E, Grote K, Kiian I, Wollert KC, Hilfiker A, Drexler H.** Regulation of proangiogenic factor CCN1 in cardiac muscle: impact of ischemia, pressure overload, and neurohumoral activation. *Circulation* 109: 2227–2233, 2004.
12. **Hunt JL, Pollak MR, Denker BM.** Cultured podocytes establish a size-selective barrier regulated by specific signaling pathways and dem-

onstrate synchronized barrier assembly in a calcium switch model of junction formation. *J Am Soc Nephrol* 16: 1593–1602, 2005.
13. **Kireeva ML, Mo FE, Yang GP, Lau LF.** Cyr61, a product of a growth factor-inducible immediate-early gene, promotes cell proliferation, migration, and adhesion. *Mol Cell Biol* 16: 1326–1334, 1996.
14. **Kireeva ML, Lam SC, Lau LF.** Adhesion of human umbilical vein endothelial cells to the immediate-early gene product Cyr61 is mediated through integrin $\alpha_v\beta_3$. *J Biol Chem* 273: 3090–3096, 1998.
15. **Koop K, Eikmans M, Baelde HJ, Kawachi H, De Heer E, Paul LC, Bruijn JA.** Expression of podocyte-associated molecules in acquired human kidney diseases. *J Am Soc Nephrol* 14: 2063–2071, 2003.
16. **Koshikawa M, Mukoyama M, Mori K, Suganami T, Sawai K, Yoshioka T, Nagae T, Yokoi H, Kawachi H, Shimizu F, Sugawara A, Nakao K.** Role of p38 mitogen-activated protein kinase activation in podocyte injury and proteinuria in experimental nephrotic syndrome. *J Am Soc Nephrol* 16: 2690–2701, 2005.
17. **Kriz W, LeHir M.** Pathways to nephron loss starting from glomerular diseases: insights from animal models. *Kidney Int* 67: 404–419, 2005.
18. **Latinkic BV, O'Brien TP, Lau LF.** Promoter function and structure of the growth factor-inducible immediate early gene *cyr61*. *Nucleic Acids Res* 19: 3261–3267, 1991.
19. **Lau LF, Lam SC.** The CCN family of angiogenic regulators: the integrin connection. *Exp Cell Res* 248: 44–57, 1999.
20. **Le Hir M, Keller C, Eschmann V, Hahnel B, Hosser H, Kriz W.** Podocyte bridges between the tuft and Bowman's capsule: an early event in experimental crescentic glomerulonephritis. *J Am Soc Nephrol* 12: 2060–2071, 2001.
21. **Miner JH, Morello R, Andrews KL, Li C, Antignac C, Shaw AS, Lee B.** Transcriptional induction of slit diaphragm genes by Lmx1b is required in podocyte differentiation. *J Clin Invest* 109: 1065–1072, 2002.
22. **Mo FE, Muntean AG, Chen CC, Stolz DB, Watkins SC, Lau LF.** CYR61 (CCN1) is essential for placental development and vascular integrity. *Mol Cell Biol* 22: 8709–8720, 2002.
23. **Moeller MJ, Soofi A, Hartmann I, Le Hir M, Wiggins R, Kriz W, Holzman LB.** Podocytes populate cellular crescents in a murine model of inflammatory glomerulonephritis. *J Am Soc Nephrol* 15: 61–67, 2004.
24. **Mundel P, Reiser J, Zuniga Mejia Borja A, Pavenstadt H, Davidson GR, Kriz W, Zeller R.** Rearrangements of the cytoskeleton and cell contracts induce process formation during differentiation of conditionally immortalized mouse podocyte cell lines. *Exp Cell Res* 236: 248–258, 1997.
25. **Nagata M, Nakayama K, Terada Y, Hoshi S, Watanabe T.** Cell cycle regulation and differentiation in the human podocyte lineage. *Am J Pathol* 153: 1511–1520, 1998.
26. **Oyanagi A, Orikasa M, Kawachi H, Ito Y, Koike H, Gejo F, Shimizu F.** Crescent-forming mechanism in an irreversible Thy-1 model in rats. *Nephron* 89: 439–447, 2001.
27. **Pavenstadt H, Kriz W, Kretzler M.** Cell biology of the glomerular podocyte. *Physiol Rev* 83: 253–307, 2003.
28. **Perbal B.** CCN proteins: multifunctional signaling regulators. *Lancet* 363: 62–64, 2004.
29. **Qiu LQ, Sinniah R, Hong Hsu SI.** Downregulation of Bcl-2 by podocytes is associated with progressive glomerular injury and clinical indices of poor renal prognosis in human IgA nephropathy. *J Am Soc Nephrol* 15: 79–90, 2004.
30. **Rampino T, Gregorini M, Camussi G, Conaldi PG, Soccio G, Maggio M, Bottelli A, Dal Canton A.** Hepatocyte growth factor and its receptor Met are induced in crescentic glomerulonephritis. *Nephrol Dial Transplant* 20: 1066–1074, 2005.
31. **Reiser J, Oh J, Shirato I, Asanuma K, Hug A, Mundel TM, Honey K, Ishidoh K, Kominami E, Kreidberg JA, Tomino Y, Mundel P.** Podocyte migration during nephrotic syndrome requires a coordinated interplay between cathepsin L and α3 integrin. *J Biol Chem* 279: 34827–34832, 2004.
32. **Sawai K, Mori K, Mukoyama M, Sugawara A, Suganami T, Koshikawa M, Yahata K, Makino H, Nagae T, Fujinaga Y, Yokoi H, Yoshioka T, Yoshimoto A, Tanaka I, Nakao K.** Angiogenic protein Cyr61 is expressed by podocytes in anti-Thy-1 glomerulonephritis. *J Am Soc Nephrol* 14: 1154–1163, 2003.
33. **Sawai K, Mukoyama M, Mori K, Yokoi H, Koshikawa M, Yoshioka T, Takeda R, Sugawara A, Kuwahara T, Saleem MA, Ogawa O, Nakao K.** Redistribution of connexin43 expression in glomerular podocytes predicts poor renal prognosis in patients with type 2 diabetes and overt nephropathy. *Nephrol Dial Transplant* 21: 2472–2477, 2006.
34. **Shankland SJ, Eitner F, Hudkins KL, Goodpaster T, D'Agati V, Alpers CE.** Differential expression of cyclin-dependent kinase inhibitors in human glomerular disease: role in podocyte proliferation and maturation. *Kidney Int* 58: 674–683, 2000.
35. **Suganami T, Mukoyama M, Mori K, Yokoi H, Koshikawa M, Sawai K, Hidaka S, Ebihara K, Tanaka T, Sugawara A, Kawachi H, Vinson C, Ogawa Y, Nakao K.** Prevention and reversal of renal injury by leptin in a new mouse model of diabetic nephropathy. *FASEB J* 19: 127–129, 2005.
36. **Vaughan MR, Pippin JW, Griffin SV, Krofft R, Fleet M, Haseley L, Shankland SJ.** ATRA induces podocyte differentiation and alters nephrin and podocin expression in vitro and in vivo. *Kidney Int* 68: 133–144, 2005.
37. **Yang GP, Lau LF.** Cyr61, product of a growth factor-inducible immediate early gene, is associated with the extracellular matrix and the cell surface. *Cell Growth Differ* 2: 351–357, 1991.

Neutrophil gelatinase-associated lipocalin as the real-time indicator of active kidney damage

K Mori[1] and K Nakao[1]

[1]*Department of Medicine and Clinical Science, Kyoto University Graduate School of Medicine, Kyoto, Japan*

Neutrophil gelatinase-associated lipocalin (Ngal, 24p3, SIP24, lipocalin 2, or siderocalin) was originally purified from neutrophils, but with unknown function. Recently, it was identified that Ngal activates nephron formation in the embryonic kidney, is rapidly and massively induced in renal failure and possesses kidney-protective activity. We would like to propose that blood, urine, and kidney Ngal levels are the real-time indicators of active kidney damage, rather than one of many markers of functional nephron number (as Forest Fire Theory). Ngal is a novel iron-carrier protein exerting pleiotropic actions including the upregulation of epithelial marker E-cadherin expression, opening an exciting field in cell biology.

Kidney International (2007) **71**, 967–970. doi:10.1038/sj.ki.5002165; published online 7 March 2007

KEYWORDS: progression of renal failure; development; iron; siderophore; mesenchymal-epithelial transition; ischemia-reperfusion; gene expression

Correspondence: *K Mori, Department of Medicine and Clinical Science, Kyoto University Graduate School of Medicine, 54 Shogoin Kawahara-cho, Sakyo-ku, Kyoto 606-8507, Japan. E-mail: keyem@kuhp.kyoto-u.ac.jp*

Received 5 December 2006; revised 4 January 2007; accepted 9 January 2007; published online 7 March 2007

MOLECULAR STRUCTURE OF NGAL

Neutrophil gelatinase-associated lipocalin (Ngal) belongs to the lipocalin superfamily, which are secreted or cytosolic proteins with barrel-like structure, carrying hydrophobic ligands (such as fatty acids, retinoids, and pheromones) in their core pocket.[1] Recent works have elucidated the pathophysiological roles of lipocalins in energy homeostasis. Retinol-binding protein 4 impairs insulin signaling in muscles causing insulin resistance,[2] whereas lipocalin-type (or brain) prostaglandin D synthase (β-trace) inhibits insulin-stimulated proliferation of vascular smooth muscle cells resulting in protection against atherosclerosis.[3] Mice with a null mutation in adipocyte fatty acid-binding protein 4 or adipocyte protein 2 become obese under high-fat diet but do not develop insulin resistance.[4] Little is known about the involvement of the ligands in these metabolic activities of lipocalins. Goetz *et al.*[5] carried out an epoch work of the X-ray crystallography for recombinant human Ngal protein expressed in *Escherichia coli*. They demonstrated that the ligand for Ngal is siderophore. Siderophores are a diverse group of small (1 kDa or less) non-peptide iron (Fe^{3+})-binding chemicals produced in bacteria, fungi, and plants and their mammalian version remains to be identified.[6–9] Of note, XL1-Blue strain of *E. coli* synthesizes a siderophore called enterochelin (or enterobactin), but BL21 commonly used for recombinant protein expression does not make enterochelin.[5] Probably outside the pocket, Ngal binds with gelatinase B (matrix metalloproteinase-9 or type IV collagenase) and with hepatocyte growth factor and modulates their activity.[10–12]

NGAL IN KIDNEY DEVELOPMENT

Mammalian metanephric mesenchyme and ureteric bud coordinate a complicated interaction to develop themselves into mature nephrons.[13] Barasch *et al.*[14] established an organ culture system, where isolated rat metanephric mesenchyme converts into glomeruli and proximal tubules by stimulation with condition media prepared from a mouse ureteric bud cell line. Leukemia-inhibitory factor and Ngal were the epithelial inducers purified at the protein level using this assay.[14,15] Genetic inactivation of Ngal (by Flo *et al.*) or leukemia-inhibitory factor signal transducer gp130 does not result in agenesis of the kidney, indicating a high redundancy in nephrogenesis pathways.[14,16] Yang *et al.*[15] have shown that

mouse Ngal protein secreted from cultured ureteric bud cells possesses nephron-inducing activity and can also bind iron. Surprisingly, Ngal–bacterial siderophore–iron complex has much stronger activity than Ngal–siderophore (without iron) and apo-Ngal (without siderophore),[17] indicating the first example of 'siderophore-binding proteins,' in any species, dependent on the presence of iron for the biological activity.[7]

NGAL IN RENAL FAILURE

Recapture of genetic program of embryo is often observed in tissue injuries. Devarajan *et al.*[18,19] have analyzed animal models of acute renal failure to screen biomarkers useful in the clinical settings and to understand the molecular mechanisms of kidney injury, to begin with by use of microarray. Within a few hours, Ngal mRNA is highly upregulated after kidney injury, such as renal ischemia-reperfusion and cisplatin nephropathy, where Ngal induction precedes the elevation of classical markers for kidney damage: serum creatinine, urinary *N*-acetyl glucosaminidase, β 2-microglobulin levels.[19,20] Furthermore, Mori *et al.*[9] and other groups have reported that Ngal protein is abundantly accumulated in the blood, urine, and renal proximal and distal tubules in acute renal failure of humans: in cases associated with renal ischemia (sepsis, hypovolemia, and heart failure), nephrotoxin (antibiotics, cisplatin, bisphosphonate, nonsteroidal anti-inflammatory drugs, radiocontrast, and hemoglobinuria), kidney-parenchymal damage (glomerulonephrits, minimal change disease, focal segmental glomerulosclerosis, and diabetic nephropathy), hemolytic-uremic syndrome and posttransplant rejection. Mishra *et al.*[21] presented the clinical usefulness of blood and urinary Ngal as extremely early markers of acute kidney disease. As early as 1–2 h after the cardiopulmonary bypass surgery in children and in adults (with average bypass time of 2–3 h), the Ngal levels are dramatically and specifically elevated in those who are going to develop acute renal failure (diagnosed by more than 50% rise in the serum creatinine levels a few days later).[21,22] Acute worsening of chronic renal failure may be also predicted by elevated urinary Ngal levels (Nickolas T *et al.*, submitted). In general, to evaluate the severity of renal failure, at least two aspects should be considered (Figure 1): the ratio of functional versus atrophic nephrons (or the results of kidney injury) and the severity of on-going damage. Analogy may hold true for forest fire (Forest Fire Theory). We propose here that induction of Ngal expression is a real-time indicator of active renal injury.

Functional significance of Ngal upregulation in renal failure was investigated by Mori[9] and Mishra *et al.*,[23] who analyzed separate sets of animals. Single intraperitoneal or subcutaneous injection of recombinant Ngal protein into mice (Figure 2) significantly ameliorates kidney damage after renal ischemia-reperfusion injury, if Ngal is given before ischemia or 1 h after reperfusion. Berger *et al.*[24] generated Ngal knockouts and found no difference in renal damage at 24 h after renal ischemia-reperfusion compared with wild-type mice. Although Ngal mRNA upregulation is a rapid response, the speed and amount of endogenous Ngal induction may not be sufficient to show significant protection in this setting. Experiments in more chronic and milder models may give different results.

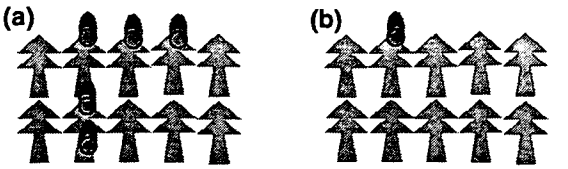

Figure 1 | Forest Fire Theory for worsening renal function. Forest (kidney) is composed of trees (nephrons). Both models (**a**) and (**b**) have 60% viable trees (shown in green) and 40% of trees are burnt down (shown in gray, corresponding to sclerosis of glomeruli, and atrophy of tubules). However, model (**a**) has much stronger fire (shown in red, that is ongoing nephron damage) than model (**b**). We propose that serum creatinine level or glomerular filtration rate is a marker for functional nephron numbers (green trees), whereas serum, urinary, or renal Ngal level indicates the extent of active lesion in the kidney (red fire in the forest).

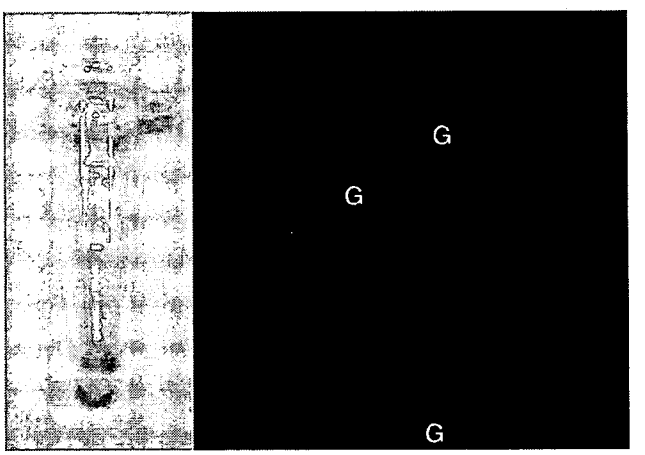

Figure 2 | Kidney protection by a red protein. Ngal protein shows a red color when ligated with iron and siderophore (left). Intravenous injection of A568-labeled Ngal (red fluorescence, right) into normal mice results in rapid glomerular (G) filtration and reabsorption by proximal tubules. Administration of iron-loaded Ngal protects the kidney from renal ischemia-reperfusion injury.

TRANSCRIPTIONAL REGULATION OF NGAL

Neutrophils,[25] monocytes/macrophages,[26] and adipocytes[27] are cells with abundant Ngal expression (Figure 3). Importantly, immature neutrophils (myelocytes and metamyelocytes) have high expression level of Ngal mRNA, whereas mature neutrophils/granulocytes in the circulation have lost the mRNA but contain large amount of Ngal protein,[25] making it impossible to determine the involvement of neutrophil-derived Ngal in tissue injury by *in situ* mRNA hybridization. Ngal expression is highly induced not only in kidney injury, but also in epithelial inflammation of intestine,[28] skin and airway,[29] and in bacterial infection[16] and cancer.[30] Ngal inducers so far identified *in vitro* are

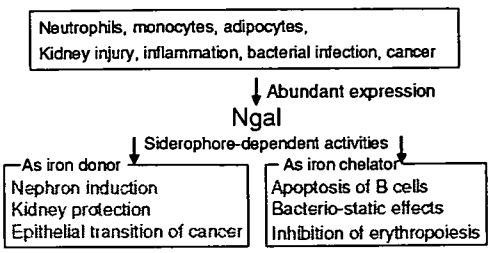

Figure 3 | Summary of expressional regulation and biological activities of Ngal.

IL-1β, tissue necrosis factor α, lipopolysaccharide, basic fibroblast growth factor, prostaglandin F2 α, phorbol ester, dexamethasone, retinoic acid, serum, and hypoxia.[20,26,29,31]

BIOLOGICAL ACTIVITY OF NGAL

Ngal exerts a broad range of biological activities (Figure 3). The coexistence of siderophore and iron is required not only for mesenchymal–epithelial transition of embryonic kidney[17] and oncogene Ras-transformed epithelial cells by Hanai *et al.*,[30] but also for kidney protection from renal failure by Mori *et al.*[9] In contrast, Ngal–siderophore complex without iron[17] (and potentially apo-Ngal)[32] can chelate iron from cells and iron deprivation is the mechanism for apoptosis of pro-B cells,[32,33] and for inhibition of bacterial growth and erythropoiesis.[5,16,34] Various other activities of Ngal are increasingly reported.[12,28]

Induction of mesenchymal–epithelial transition by Ngal is associated with upregulation of epithelial marker E-cadherin expression, but this is a slow process. In metanephric mesenchyme, morphologically distinct epithelia is observed only 7–10 days after addition of Ngal–siderophore–iron complex (unpublished observation).[15] By contrast, epithelia induced by leukemia-inhibitory factor can be observed within 4–5 days.[13,14] In Ras-transformed mammary cells, E-cadherin protein accumulation was evaluated 48 h after treatment with the complex.[30] Hanai *et al.*[30] demonstrated that treatment with Ngal–siderophore–iron suppresses Raf, mitogen-activated protein kinase (MEK)-1/2, extracellular signal-regulated kinase (ERK)-1/2 pathway of mitogen-activated protein kinase and inhibits E-cadherin phosphorylation, causing decrease in E-cadherin degradation. Not only treatment with Ngal–siderophore–iron complex but also transfection with cDNA and infection with adenovirus encoding Ngal results in mesenchymal–epithelial transition of transformed cells, implying that fetal calf serum or cells themselves provide mammalian siderophores. In the case of renal ischemia-reperfusion injury, phosphorylation of MEK1/2 and ERK1/2 is biphasic (transient activation within 30 min, followed by long-term activation for several days) and the levels of their phosphorylation are not necessarily parallel with the severity of renal injury,[35] suggesting that suppression of this pathway is not the major mechanism for Ngal-mediated kidney protection. Administration of Ngal is ineffective if given 2 h after reperfusion,[9] implying that Ngal is preventing the early injuries (in part by upregulating a protective enzyme heme oxygenase-1)[9] rather than stimulating the recovery process.

In healthy adult kidneys, Ngal[36] and other lipocalins (whose sizes are 17–43 kDa) including retinol-binding protein 4, α1-microglobulin[37] and probably also liver-type fatty acid-binding protein 1 and prostaglandin D synthase are freely filtrated in the glomeruli, bound to multiligand scavenger-receptor megalin (expressed abundantly and specifically on the brush borders of proximal tubules) and taken up efficiently by endocytosis (as well as albumin and β2-microglobulin).[38] Insufficient tubular reabsorption (owing to specific saturation in the endocytic pathway or general malfunctioning of proximal tubules) should contribute in part to urinary Ngal. Devireddy *et al.*[32] identified brain-type organic cation transporter as Ngal receptor in pro-B cells.

Iron-free siderophore-like activity (which assists the binding of Ngal and Fe^{3+}) is detectable in the normal urine of humans, mice, rats, and dogs.[9,39] Tear lipocalin, a major protein component specifically found in human tears, also binds with siderophores.[40] Lipocalin 12, found specifically in mouse epididymis, is also structurally related to Ngal and may have binding capacity for siderophores.[41]

CHARACTERISTICS OF NGAL AS RENAL FAILURE BIOMARKER

Ngal induction is a rapid event detectable within a few hours, characterizing Ngal as one of immediate early genes or acute-phase reactants such as IL-6 and C-reactive protein. Fold induction of Ngal mRNA and protein is log order of magnitude, reaching 1000-fold in most severe cases of renal injury.[9,39] Therefore, normalization for urinary creatinine level is not necessary to evaluate urinary Ngal.[21] Indeed, a patient with urinary Ngal level of 40 μg/ml died of multi-organ failure 12 h after urine collection[9] (Mori K *et al.*, unpublished observation).

DIRECTIONS FOR FUTURE RESEARCH

There are a number of siderohpre-dependent and -independent activities reported for Ngal. The role of endogenously expressed Ngal in these activities should be better verified using Ngal-deficient mice. During renal ischemia-reperfusion injury, the liver also starts to express Ngal mRNA.[39] Therefore, the source of Ngal protein in the blood and urine during renal injury can be a complex from the kidney, liver, and white blood cells (in the injured tissues and in circulation). Tissue-specific disruption of Ngal gene will make it possible to investigate what is the predominant source of Ngal, as a biomarker or as a protective mechanism for renal failure. Purification and identification of mammalian siderophores and to learn their metabolism and regulation are also important steps. The reported method to recognize siderophores is only available for iron-free molecules.[9] A new way to detect iron-loaded siderophores must be invented. Characterization of Ngal receptors, their downstream intracellular signaling, and subcellular localization of events will help elucidate the

detailed molecular mechanism underlying the actions of Ngal, siderophores, and iron.

CONCLUSION

Ngal is a very unique protein endowed with iron-carrying activity and diagnostic and therapeutic utilities for renal failure, which is acquiring an explosion of attention by researchers and clinicians beyond nephrology.

ACKNOWLEDGMENTS

Unfortunately, we could not describe all the contributors and original papers in Ngal research. We thank Drs. J Barasch, P Devarajan, and Q Al-awqati for discussion, instruction, and encouragement. We are also grateful to Drs. J Yang, KM Schmidt-Ott, JY Li, N Paragas, A Kalandadze, HT Lee, FH Cheema (Columbia University), and M Mukoyama, M Kasahara, H Yokoi, K Sawai, T Suganami, and T Kuwabara (Kyoto University). This work was supported by grants from Uehara Memorial Foundation, Yamanouchi Foundation for Research on Metabolic Disorders, Salt Science Research Foundation, Japanese Ministry of Education, Culture, Sports, Science and Technology, and from Japan Society for Promotion of Science.

REFERENCES

1. Flower DR, North AC, Sansom CE. The lipocalin protein family: structural and sequence overview. *Biochim Biophys Acta* 2000; **1482**: 9–24.
2. Yang Q, Graham TE, Mody N *et al.* Serum retinol binding protein 4 contributes to insulin resistance in obesity and type 2 diabetes. *Nature* 2005; **436**: 356–362.
3. Ragolia L, Palaia T, Hall CE *et al.* Accelerated glucose intolerance, nephropathy, and atherosclerosis in prostaglandin D2 synthase knockout mice. *J Biol Chem* 2005; **280**: 29946–29955.
4. Hotamisligil GS, Johnson RS, Distel RJ *et al.* Uncoupling of obesity from insulin resistance through a targeted mutation in aP2, the adipocyte fatty acid binding protein. *Science* 1996; **274**: 1377–1379.
5. Goetz DH, Holmes MA, Borregaard N *et al.* The neutrophil lipocalin NGAL is a bacteriostatic agent that interferes with siderophore-mediated iron acquisition. *Mol Cell* 2002; **10**: 1033–1043.
6. Raymond KN, Dertz EA, Kim SS. Enterobactin: an archetype for microbial iron transport. *Proc Natl Acad Sci USA* 2003; **100**: 3584–3588.
7. Barasch J, Mori K. Cell biology: iron thievery. *Nature* 2004; **432**: 811–813.
8. Takahashi M, Nakanishi H, Kawasaki S *et al.* Enhanced tolerance of rice to low iron availability in alkaline soils using barley nicotianamine aminotransferase genes. *Nat Biotechnol* 2001; **19**: 466–469.
9. Mori K, Lee HT, Rapoport D *et al.* Endocytic delivery of lipocalin-siderophore-iron complex rescues the kidney from ischemia-reperfusion injury. *J Clin Invest* 2005; **115**: 610–621.
10. Kjeldsen L, Johnsen AH, Sengelov H *et al.* Isolation and primary structure of NGAL, a novel protein associated with human neutrophil gelatinase. *J Biol Chem* 1993; **268**: 10425–10432.
11. Yan L, Borregaard N, Kjeldsen L *et al.* The high molecular weight urinary matrix metalloproteinase (MMP) activity is a complex of gelatinase B/MMP-9 and neutrophil gelatinase-associated lipocalin (NGAL). Modulation of MMP-9 activity by NGAL. *J Biol Chem* 2001; **276**: 37258–37265.
12. Gwira JA, Wei F, Ishibe S *et al.* Expression of neutrophil gelatinase-associated lipocalin regulates epithelial morphogenesis *in vitro*. *J Biol Chem* 2005; **280**: 7875–7882.
13. Mori K, Yang J, Barasch J. Ureteric bud controls multiple steps in the conversion of mesenchyme to epithelia. *Semin Cell Dev Biol* 2003; **14**: 209–216.
14. Barasch J, Yang J, Ware CB *et al.* Mesenchymal to epithelial conversion in rat metanephros is induced by LIF. *Cell* 1999; **99**: 377–386.
15. Yang J, Goetz D, Li JY *et al.* An iron delivery pathway mediated by a lipocalin. *Mol Cell* 2002; **10**: 1045–1056.
16. Flo TH, Smith KD, Sato S *et al.* Lipocalin 2 mediates an innate immune response to bacterial infection by sequestrating iron. *Nature* 2004; **432**: 917–921.
17. Li JY, Ram G, Gast K *et al.* Detection of intracellular iron by its regulatory effect. *Am J Physiol Cell Physiol* 2004; **287**: C1547–C1559.
18. Devarajan P. Update on mechanisms of ischemic acute kidney injury. *J Am Soc Nephrol* 2006; **17**: 1503–1520.
19. Supavekin S, Zhang W, Kucherlapati R *et al.* Differential gene expression following early renal ischemia/reperfusion. *Kidney Int* 2003; **63**: 1714–1724.
20. Mishra J, Ma Q, Prada A *et al.* Identification of neutrophil gelatinase-associated lipocalin as a novel early urinary biomarker for ischemic renal injury. *J Am Soc Nephrol* 2003; **14**: 2534–2543.
21. Mishra J, Dent C, Tarabishi R *et al.* Neutrophil gelatinase-associated lipocalin (NGAL) as a biomarker for acute renal injury after cardiac surgery. *Lancet* 2005; **365**: 1231–1238.
22. Wagener G, Jan M, Kim M *et al.* Association between increases in urinary neutrophil gelatinase-associated lipocalin and acute renal dysfunction after adult cardiac surgery. *Anesthesiology* 2006; **105**: 485–491.
23. Mishra J, Mori K, Ma Q *et al.* Amelioration of ischemic acute renal injury by neutrophil gelatinase-associated lipocalin. *J Am Soc Nephrol* 2004; **15**: 3073–3082.
24. Berger T, Togawa A, Duncan GS *et al.* Lipocalin 2-deficient mice exhibit increased sensitivity to Escherichia coli infection but not to ischemia-reperfusion injury. *Proc Natl Acad Sci USA* 2006; **103**: 1834–1839.
25. Cowland JB, Borregaard N. The individual regulation of granule protein mRNA levels during neutrophil maturation explains the heterogeneity of neutrophil granules. *J Leukoc Biol* 1999; **66**: 989–995.
26. Meheus LA, Fransen LM, Raymackers JG *et al.* Identification by microsequencing of lipopolysaccharide-induced proteins secreted by mouse macrophages. *J Immunol* 1993; **151**: 1535–1547.
27. Wang Y, Lam KS, Kraegen EW *et al.* Lipocalin-2 is an inflammatory marker closely associated with obesity, insulin resistance, and hyperglycemia in humans. *Clin Chem* 2007; **53**: 34–41.
28. Playford RJ, Belo A, Poulsom R *et al.* Effects of mouse and human lipocalin homologues 24p3/lcn2 and neutrophil gelatinase-associated lipocalin on gastrointestinal mucosal integrity and repair. *Gastroenterology* 2006; **131**: 809–817.
29. Cowland JB, Sorensen OE, Sehested M *et al.* Neutrophil gelatinase-associated lipocalin is up-regulated in human epithelial cells by IL-1 beta, but not by TNF-alpha. *J Immunol* 2003; **171**: 6630–6639.
30. Hanai J, Mammoto T, Seth P *et al.* Lipocalin 2 diminishes invasiveness and metastasis of Ras-transformed cells. *J Biol Chem* 2005; **280**: 13641–13647.
31. Liu Q, Nilsen-Hamilton M. Identification of a new acute phase protein. *J Biol Chem* 1995; **270**: 22565–22570.
32. Devireddy LR, Gazin C, Zhu X *et al.* A cell-surface receptor for lipocalin 24p3 selectively mediates apoptosis and iron uptake. *Cell* 2005; **123**: 1293–1305.
33. Devireddy LR, Teodoro JG, Richard FA *et al.* Induction of apoptosis by a secreted lipocalin that is transcriptionally regulated by IL-3 deprivation. *Science* 2001; **293**: 829–834.
34. Miharada K, Hiroyama T, Sudo K *et al.* Lipocalin 2 functions as a negative regulator of red lood cell production in an autocrine fashion. *FASEB J* 2005; **19**: 1881–1883.
35. Park KM, Kramers C, Vayssier-Taussat M *et al.* Prevention of kidney ischemia/reperfusion-induced functional injury MAPK and MAPK kinase activation, and inflammation by remote transient ureteral obstruction. *J Biol Chem* 2002; **277**: 2040–2049.
36. Hvidberg V, Jacobsen C, Strong RK *et al.* The endocytic receptor megalin binds the iron transporting neutrophil-gelatinase-associated lipocalin with high affinity and mediates its cellular uptake. *FEBS Lett* 2005; **579**: 773–777.
37. Leheste JR, Rolinski B, Vorum H *et al.* Megalin knockout mice as an animal model of low molecular weight proteinuria. *Am J Pathol* 1999; **155**: 1361–1370.
38. Moestrup SK, Verroust PJ. Megalin- and cubilin-mediated endocytosis of protein-bound vitamins, lipids, and hormones in polarized epithelia. *Annu Rev Nutr* 2001; **21**: 407–428.
39. Schmidt-Ott KM, Mori K, Kalandadze A *et al.* Neutrophil gelatinase-associated lipocalin-mediated iron traffic in kidney epithelia. *Curr Opin Nephrol Hypertens* 2006; **15**: 442–449.
40. Fluckinger M, Haas H, Merschak P *et al.* Human tear lipocalin exhibits antimicrobial activity by scavenging microbial siderophores. *Antimicrob Agents Chemother* 2004; **48**: 3367–3372.
41. Holmes MA, Paulsene W, Jide X *et al.* Siderocalin (Lcn 2) also binds carboxymycobactins, potentially defending against mycobacterial infections through iron sequestration. *Structure* 2005; **13**: 29–41.

DEVELOPMENTAL DYNAMICS 236:2779–2791, 2007

RESEARCH ARTICLE

Rbp-j Regulates Expansion of Pancreatic Epithelial Cells and Their Differentiation Into Exocrine Cells During Mouse Development

Junji Fujikura,[1] Kiminori Hosoda,[1]* Yoshiya Kawaguchi,[2] Michio Noguchi,[1] Hiroshi Iwakura,[1] Shinji Odori,[1] Eisaku Mori,[1] Tsutomu Tomita,[1] Masakazu Hirata,[1] Ken Ebihara,[1] Hiroaki Masuzaki,[1] Akihisa Fukuda,[2,3] Kenichiro Furuyama,[2] Kenji Tanigaki,[4] Daisuke Yabe,[5] and Kazuwa Nakao[1]

Notch signaling regulates cell fate determination in various tissues. We have reported the generation of mice with a pancreas-specific knockout of Rbp-j using *Pdx.cre* mice. Those mice exhibited premature endocrine and ductal differentiation. We now generated mice in which the *Rbp-j* gene was inactivated in Ptf1a-expressing cells using *Ptf1a.cre* mice. The timing of the Cre-mediated deletion in *Rbp-j$^{f/f}$ Ptf1a.cre* mice is 1 day later than that in *Rbp-j$^{f/f}$ Pdx.cre* mice. In *Rbp-j$^{f/f}$ Ptf1a.cre* mouse pancreases, at E13.5, the reduced Hes1 expression was accompanied by reduced epithelial growth, but premature endocrine cell differentiation was minimal. At E15.5, Pdx1 expression was repressed and acinar cell differentiation was reduced, but an increase in acinar cell proliferation was observed during the perinatal period. Our study indicates that, in addition to its role in preventing premature differentiation of early endocrine cells, Rbp-j regulates epithelial growth, Pdx1 expression, and acinar cell differentiation during mid-pancreatic development. *Developmental Dynamics 236:2779–2791, 2007.* © 2007 Wiley-Liss, Inc.

Key words: pancreatic development; Rbp-j; Notch signaling; Pdx1; Ptf1a; conditional knockout (KO) mice

Accepted 26 July 2007

INTRODUCTION

The pancreas plays a key role in the maintenance of nutritional homeostasis through its exocrine and endocrine functions. The exocrine acini secrete digestive enzymes into the duodenum through ducts, whereas the endocrine cells in the islets produce peptide hormones (Heller et al., 2005). Notch signaling regulates various developmental processes, such as neurogenesis, somitogenesis, angiogenesis, and hematopoiesis (Ishibashi et al., 1995; Hrabé de Angelis et al., 1997; Xue et al., 1999; Han et al., 2002). The interaction of a Notch receptor with its ligand induces the cleavage of the receptor's intracellular domain (Notch ICD), which translocates to the nucleus and binds to Rbp-j to induce the expression of the Hes family of transcriptional repressors (Kageyama and Ohtsuka, 1999). Rbp-j is a key mediator of Notch signaling, because it is expressed ubiquitously and associates with all four types of Notch receptors (Kato et al., 1996; Beres et al., 2006). Various Notch-related genes are expressed in the developing pancreas (Lammert et al., 2000). However, multiple anomalies and early embryonic deaths of mice with homozygous deletions of such genes limit the possible

The Supplementary Material referred to in this article can be found at http://www.interscience.wiley.com/jpages/1058-8388/suppmat

[1]Department of Medicine and Clinical Science, Kyoto University Graduate School of Medicine, Sakyo-ku, Kyoto, Japan
[2]Department of Surgery and Surgical Basic Science, Kyoto University Graduate School of Medicine, Sakyo-ku, Kyoto, Japan
[3]Department of Gastroenterology and Hepatology, Kyoto University Graduate School of Medicine, Sakyo-ku, Kyoto, Japan
[4]Research Institute, Shiga Medical Center, Moriyama, Shiga, Japan
[5]Department of Medical Chemistry, Kyoto University Graduate School of Medicine, Yoshida-Konoe-cho, Sakyo-ku, Kyoto, Japan

Grant sponsor: the Ministry of Education, Culture, Sports, Science, and Technology of Japan; Grant number: Grant-in-aid; Grant sponsor: The Smoking Research Foundation.

***Correspondence to: Kiminori Hosoda, Department of Medicine and Clinical Science, Kyoto University Graduate School of Medicine, 54 Shogoin Kawahara-cho, Sakyo-ku, Kyoto 606-8507, Japan. E-mail: pekopaokuro@yahoo.co.jp**

DOI 10.1002/dvdy.21310
Published online 7 September 2007 in Wiley InterScience (www.interscience.wiley.com).

assessment of the importance of Notch signaling in this organ (Swiatek et al., 1994; Ishibashi et al., 1995; Oka et al., 1995; Hrabé de Angelis et al., 1997; Xue et al., 1999; Apelqvist et al., 1999; Hamada et al., 1999; Jensen et al., 2000). We recently reported the generation of mice in which the *Rbp-j* gene is inactivated by Cre recombinase under the control of the *Pdx1* promoter (*Rbp-j$^{f/f}$ Pdx.cre* mice; Fujikura et al., 2006). Pdx1 is a homeobox transcription factor required for pancreatic outgrowth and the differentiation of the rostral duodenum (Offield et al., 1996). This protein is first detected in the endodermal domains of the foregut–midgut junction from as early as embryonic day (E) 8.5 (Guz et al., 1995; Offield et al., 1996; Edlund, 2002). In *Rbp-j$^{f/f}$ Pdx.cre* mice, the premature differentiation of pancreatic progenitor cells into endocrine and ductal cells leads to pancreatic hypoplasia and insulin-deficient diabetes mellitus. Ptf1a, like Pdx1, is a transcription factor that is expressed in pancreatic progenitors of exocrine, endocrine, and duct cells within the pancreatic buds of the early embryo. Ptf1a is a basic helix–loop–helix type of transcription factor, which is necessary for pancreatic specification and early organogenesis (Cockell et al., 1989; Kawaguchi et al., 2002). Ptf1a protein can be found at E10.5, shortly after the onset of endodermal budding, only in the cells that become committed to pancreatic fates (Hald et al., 2003). In this study, to further elucidate the role of Rbp-j–mediated Notch signaling in the developing pancreas using the different times of expression of Ptf1a and Pdx1, we disrupted Rbp-j with Cre recombinase under the control of the endogenous Ptf1a promoter. In *Rbp-j$^{f/f}$ Ptf1a.cre* mouse pancreases, the number of Hes1-positive cells decreased, but premature endocrine or ductal differentiation was minimal. The branching morphogenesis of the epithelium and acinar cell differentiation were disturbed with reduced Pdx1 expression in the mutant pancreases. Our study indicates that Rbp-j regulates epithelial growth, Pdx1 expression, and acinar cell differentiation during mid-pancreatic development.

RESULTS

Timing of Cre/loxP Recombination in *Rbp-j$^{f/f}$ Ptf1a.cre* Mice Is Developmentally Later Than That in *Rbp-j$^{f/f}$ Pdx.cre* Mice

To study the role of Rbp-j in pancreatic development and function, we conditionally deleted the gene for Rbp-j in the developing pancreas. In the floxed allele of *Rbp-j*, loxP sites were introduced upstream from exon 6 and downstream from exon 7 of the gene (Han et al., 2002). Exons 6 and 7 encode DNA-binding and Notch-binding domains, and the lack of these exons results in the complete loss of Rbp-j–mediated Notch signaling. *Rbp-j^{f}* is a very efficient target for Cre recombinase in multiple tissues (Han et al., 2002; Tanigaki et al., 2002, 2004; Yamamoto et al., 2003; Fujikura et al., 2006; Buono et al., 2006). Recently, we reported the generation of mice in which the *Rbp-j* gene was inactivated by Cre recombinase under the control of the *Pdx1* promoter (*Rbp-j$^{f/f}$ Pdx.cre*; Fujikura et al., 2006). We next mated *Rbp-j$^{f/f}$* mice with mice expressing Cre recombinase driven by the endogenous Ptf1a promoter (*Rbp-j$^{f/f}$ Ptf1a.cre*; Kawaguchi et al., 2002). We monitored the timing of Cre/loxP recombination using Rosa26-lacZ reporter (*Rosa26R*) mice. The *Rosa26R* allele carries a histochemical marker *lacZ* gene driven by the promoter of the ubiquitously expressed *Rosa26* gene in a configuration such that transcription is terminated upstream from the *lacZ* reporter by floxed stop sequences (Soriano, 1999). To visualize the Cre-mediated loxP recombination, mice heterozygous for floxed *Rbp-j* and homozygous for the *Rosa26R* allele, *Rosa26R$^{f/f}$ Rbp-j$^{f/+}$* were crossed with double heterozygous *Rbp-j$^{f/+}$ Ptf1a.cre* or *Rbp-j$^{f/+}$ Pdx.cre* mice. In the offspring, the expression of Cre recombinase excises both the stop cassette upstream from the *lacZ* gene and the genomic region from exons 6 to 7 of the *Rbp-j* gene, thereby activating the expression of β-galactosidase and inactivating that of Rbp-j. Because recombination is never reversed, *lacZ* expression persists in all descendants of the cells in which the *Rbp-j* gene is deleted from the genome. X-gal (5-Bromo-4-chloro-3-indolyl-β-D-galactoside) staining of *Rosa26R$^{f/+}$ Rbp-j$^{f/f}$ Pdx.cre* embryos appeared between somite stages 19 and 22 (E9.5) in the dorsal and ventral pancreatic buds of the foregut region (Fig. 1, upper panels). However, in the *Rosa26R$^{f/+}$ Rbp-j$^{f/f}$ Ptf1a.cre* embryos, X-gal staining first appeared somite stage 32 or 33 (E10.5) in the dorsal and ventral pancreatic buds (Fig. 1, lower panels). Thus, the timing of the gene deletion in the *Rbp-j$^{f/f}$ Ptf1a.cre* mice was approximately 1 day later developmentally than that in the *Rbp-j$^{f/f}$ Pdx.cre* mice. At various developmental stages in *Rosa26R$^{f/+}$ Rbp-j$^{f/+}$ Ptf1a.cre* and *Rosa26R$^{f/+}$ Rbp-j$^{f/f}$ Ptf1a.cre* mice, we generally detected uniform β-galactosidase activity throughout the pancreatic tissues (Supplementary Figure S1A–1E, which can be viewed at http://www.interscience.wiley.com/jpages/1058-8388/suppmat), but not in early glucagon-producing cells (Supplementary Figure S1C).

A paralog of Rbp-j, Rbp-L is expressed in pancreatic acinar cells (Minoguchi et al., 1997; Beres et al., 2006). The Rbp-L protein binds to a DNA sequence almost identical to that of Rbp-j, but does not interact with any of the four known mammalian Notch receptors (Minoguchi et al., 1997). No compensatory up-regulation of Rbp-L could be detected by immunostaining with specific antibody (Supplementary Figure S2).

Decreased Epithelial Cell Proliferation and Reduced Branching Morphogenesis in the Pancreases of *Rbp-j$^{f/f}$ Ptf1a.cre* Mice at E13.5

At E13.5, the Pdx1-positive pancreatic epithelium of the control mice had already started to branch (Fig. 2Aa). However, in *Rbp-j$^{f/f}$ Ptf1a.cre* mice, the Pdx1-positive epithelium rarely branched, and dilated tubular structures were prominent (Fig. 2Ab). In the control pancreas, Hes1 expression was broadly distributed in the branching epithelium (Fig. 2Ac) and neurogenin 3 expression was mainly detected in cells located in the central region of the epithelium (Fig. 2Ae). In the mutant pancreas, the ratio of Hes1-positive cells to Pdx1-positive cells (Hes1+/Pdx1+) significantly de-

creased to 55% of the control (*Rbp-j$^{f/+}$ Ptf1a.cre*, 24.1 ± 2.5 vs. *Rbp-j$^{f/f}$ Ptf1a.cre*, 13.3 ± 1.7%; $P = 0.01$; Fig. 2Ac,Ad,B), and neurogenin 3+/Pdx1+ ratio increased to 112% of the control, but was not significant (*Rbp-j$^{f/+}$ Ptf1a.cre*, 5.1 ± 0.4 vs. *Rbp-j$^{f/f}$ Ptf1a.cre*, 5.8 ± 0.8%; $P = 0.42$; Fig. 2Ae,Af,B). Most of the cells in the dilated tubular structures stained negatively for both Hes1 (Fig. 2Ad) and neurogenin 3 (Fig. 2Af). Synaptophysin is a marker for neuroendocrine cells (Wiedenmann et al., 1986). Synaptophysin-positive cell clusters were observed in both the control and mutant pancreases (Fig. 2Ag,Ah). Lineage tracing experiments showed that these large clusters were mainly composed of glucagon-expressing cells retaining unrecombined allele (Supplementary Figure S1C). However, synaptophysin+/ Pdx1+ ratio increased to 186% of the control (*Rbp-j$^{f/+}$ Ptf1a.cre*, 5.2 ± 1.0 vs. *Rbp-j$^{f/f}$ Ptf1a.cre*, 9.8 ± 1.6%; $P = 0.04$; Fig. 2Ag,Ah,B), reflecting to some extent the decreased number of Pdx1-positive cells (Fig. 2Ab). The expression of carboxypeptidase A, an earlier exocrine cell marker than amylase (Gittes and Rutter, 1992), was detected peripherally at the tip of the branches in the control pancreas (Fig. 2Ai). In contrast, carboxypeptidase-A–expressing cells were rarely found in the mutant (Fig. 2Aj). Reduced outgrowth and branching of the epithelium in the mutant was accompanied by a decrease in the number of proliferating cells detected by phospho-histone H3 immunostaining (Fig. 2Ak,Al). The phospho-histone H3+/ Pdx1+ ratio decreased to 40% of the control (*Rbp-j$^{f/+}$ Ptf1a.cre*, 4.4 ± 0.6 vs. *Rbp-j$^{f/f}$ Ptf1a.cre*, 1.8 ± 0.5%; $P =$

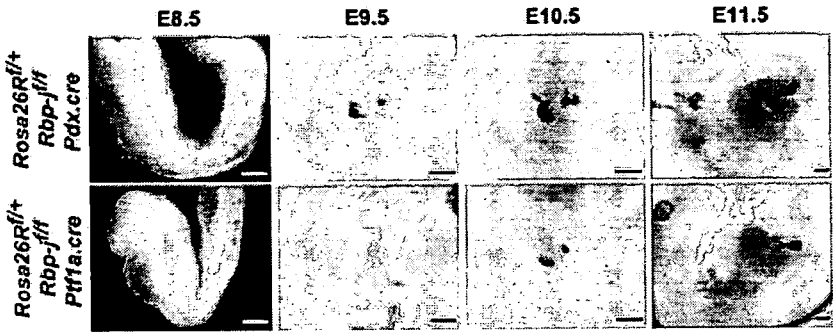

Fig. 1. Timing of Cre/loxP recombination in *Rbp-j$^{f/f}$ Ptf1a.cre* mice is later developmentally than in *Rbp-j$^{f/f}$ Pdx.cre* mice. X-gal staining of whole embryos from *Rosa26R$^{f/+}$ Rbp-j$^{f/f}$ Pdx.cre* mice (upper panels) and *Rosa26R$^{f/+}$ Rbp-j$^{f/f}$ Ptf1a.cre* mice (lower panels) at embryonic days (E) 8.5, E9.5, E10.5, and E11.5. *Pdx.cre*-mediated recombination is first detected at E9.5, but *Ptf1a.cre*-mediated recombination is first detected at E10.5. Scale bars = 200 μm.

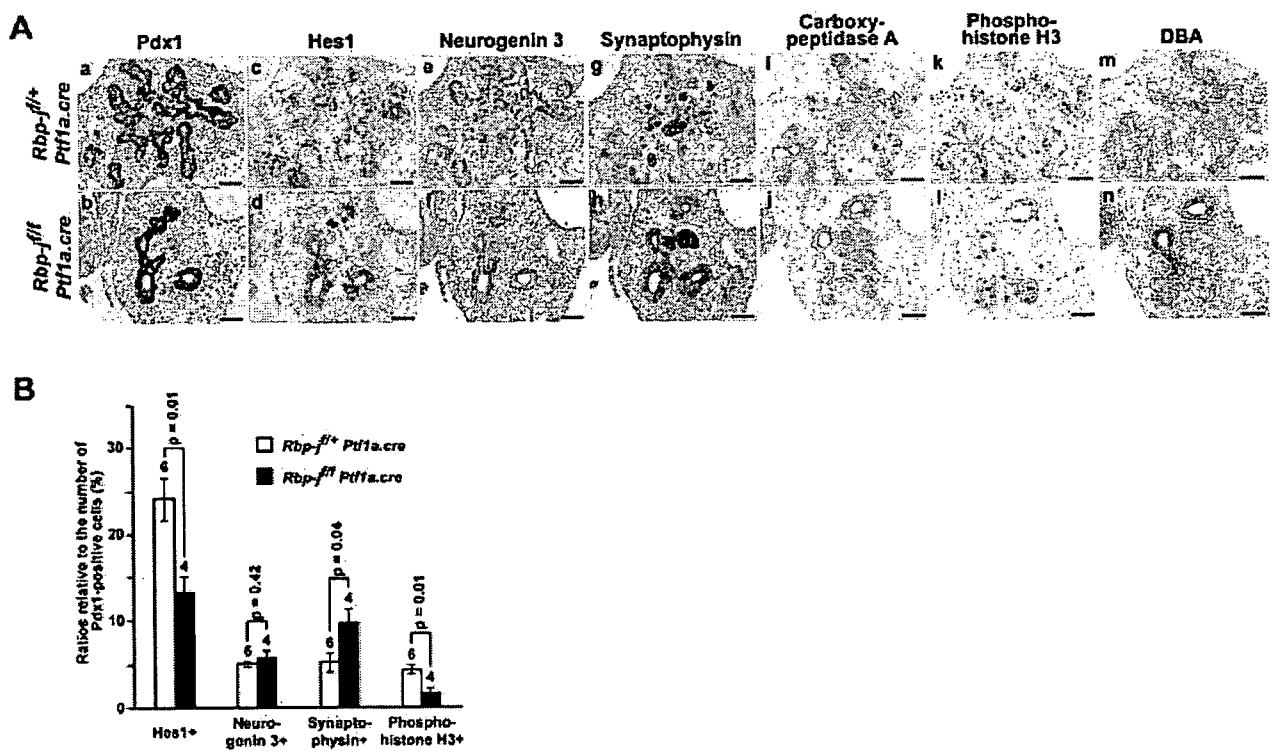

Fig. 2. Decreased epithelial cell proliferation and reduced branching morphogenesis in the pancreases of *Rbp-j$^{f/f}$ Ptf1a.cre* mice at embryonic day (E) 13.5. A: Immunohistochemistry of Pdx1 (a,b), Hes1 (c,d), neurogenin 3 (e,f), synaptophysin (g,h), carboxypeptidase A (i,j), phospho-histone H3 (k,l), Dolichos biflorus agglutinin (DBA; m,n) using serial pancreatic sections from *Rbp-j$^{f/+}$ Ptf1a.cre* and *Rbp-j$^{f/f}$ Ptf1a.cre* mice at E13.5. B: The relative numbers of Hes1, neurogenin 3, synaptophysin, and phospho-histone H3–positive cells to Pdx1-positive cells. Standard errors and number of mice examined are indicated on the average bars. Levels of significance (Student's *t*-tests) are shown. In the mutant pancreas, epithelial growth and branching is significantly reduced. Scale bars = 50 μm.

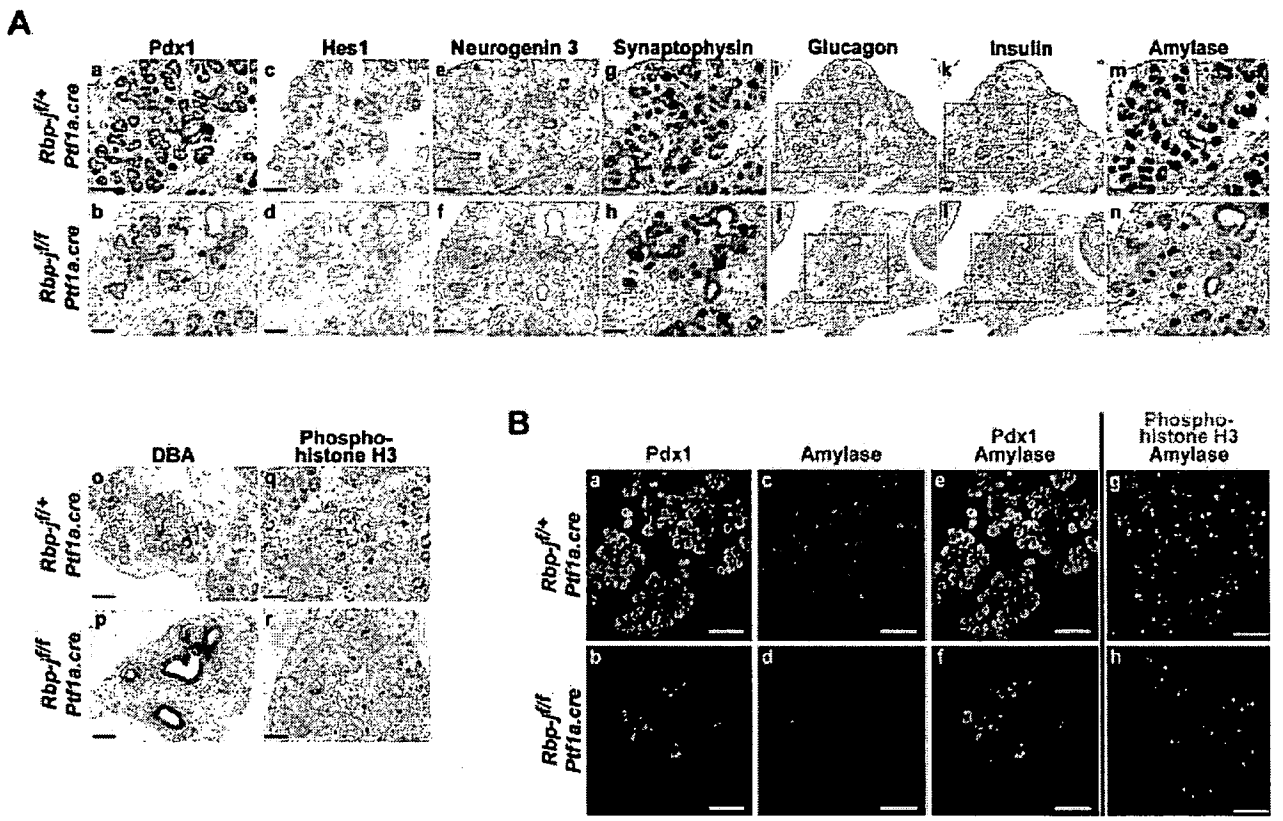
A
Pdx1
Hes1
Neurogenin 3
Synaptophysin
Glucagon
Insulin
Amylase
Rbp-j f/+ Ptf1a.cre
Rbp-j f/f Ptf1a.cre
DBA
Phospho-histone H3
B
Pdx1
Amylase
Pdx1 Amylase
Phospho-histone H3 Amylase

Fig. 3.

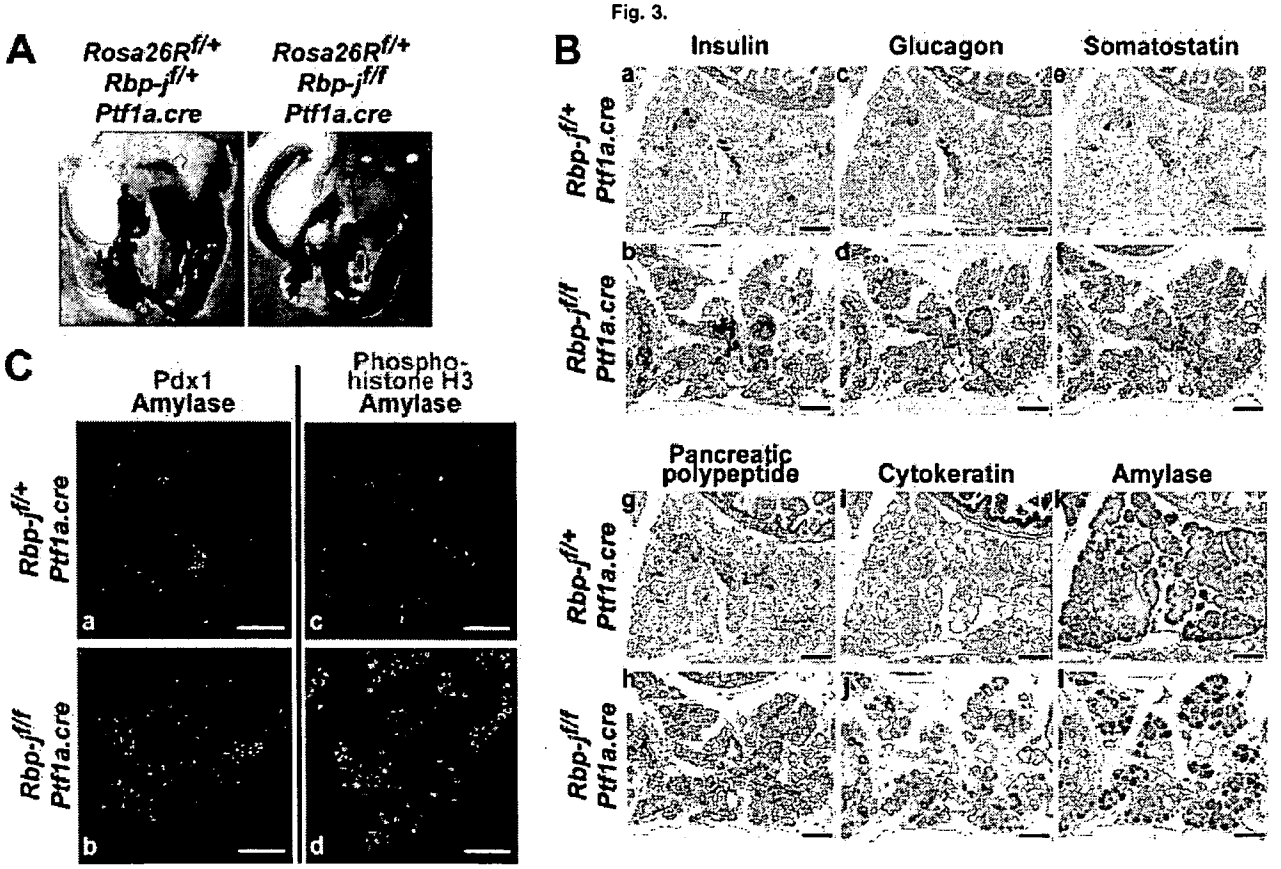
A
Rosa26R f/+ Rbp-j f/+ Ptf1a.cre
Rosa26R f/+ Rbp-j f/f Ptf1a.cre
B
Insulin
Glucagon
Somatostatin
Pancreatic polypeptide
Cytokeratin
Amylase
C
Pdx1 Amylase
Phospho-histone H3 Amylase

Fig. 4.